J. Fluid Mech. (1987), *vol.* 185, *pp.* 289–321
Printed in Great Britain

Bubble dynamics in a compressible liquid. Part 2. Second-order theory

By A. LEZZI AND A. PROSPERETTI†
Department of Mechanical Engineering, The Johns Hopkins University, Baltimore, MD 21218, USA

(Received 9 May 1986 and in revised form 27 May 1987)

The radial dynamics of a spherical bubble in a compressible liquid is studied by means of a rigorous singular-perturbation method to second order in the bubble-wall Mach number. The results of Part 1 (Prosperetti & Lezzi, 1986) are recovered at orders zero and one. At second order the ordinary inner and outer structure of the solution proves inadequate to correctly describe the fields and it is necessary to introduce an intermediate region the characteristic length of which is the geometric mean of the inner and outer lengthscales. The degree of indeterminacy for the radial equation of motion found at first order is significantly increased by going to second order. As in Part 1 we examine several of the possible forms of this equation by comparison with results obtained from the numerical integration of the complete partial-differential-equation formulation. Expressions and results for the pressure and velocity fields in the liquid are also reported.

1. Introduction

In a preceding paper (Prosperetti & Lezzi 1986, hereinafter referred to as I) the problem of the derivation of an approximate equation for the radial motion of a bubble in a compressible liquid was considered. Use was made of a simplified version of the method of matched asymptotic expansions and results valid to first order in the Mach number of the flow were obtained. An attempt to proceed to the next step in the perturbation solution by the same method fails because of its inadequacy to handle the complex mathematical structure which appears at the second order. In the present paper we make use of a more sophisticated version of the matched asymptotic expansion technique and succeed in obtaining an equation of motion for the bubble radius valid to second order in the Mach number. This equation is actually a two-parameter family. The same non-uniqueness problem encountered in I appears, compounded by the presence of an extra degree of freedom at the next order. Furthermore, no indication as to which of the first-order equations is to be preferred can be obtained by an examination of the second-order results. In the same spirit as in I we consider numerical solutions of the exact partial differential formulation of the problem in an attempt to discriminate among the possible equations.

While up to the first order in the Mach number the solution has the customary structure of an inner and an outer expansion, it is found that at the second order an intermediate region arises from the outer field and acts as a sort of buffer between it and the inner one. Proper inclusion of this solution is essential for matching and the

† Present address: Dipartimento di Matematica, Universitá degli Studi, Cagliari, Italy.

correct determination of the fields although, if one were to proceed blindly ignoring this problem, the same equation of motion for the bubble radius would be found. A situation similar to the one encountered here arises in the theory of aerodynamic sound generation by the flow of a compressible fluid (Obermeier 1976). The ideas of Kaplun (1967) on limit equations and matching (see also Lagerstrom & Casten 1972) furnish, here as in that problem, the key to the correct solution.

2. Mathematical formulation

We summarize here the mathematical formulation derived in I. In terms of the velocity potential φ the equation of continuity is

$$\nabla^2\varphi+\frac{1}{c^2}\left(\frac{\partial h}{\partial t}+\frac{\partial\varphi}{\partial r}\frac{\partial h}{\partial r}\right)=0, \tag{2.1}$$

where $c^2 = \mathrm{d}p/\mathrm{d}\rho$ is the speed of sound in the liquid and

$$h=\int_{p_\infty}^{p}\frac{\mathrm{d}p}{\rho}, \tag{2.2}$$

is the liquid enthalpy referred to the undisturbed pressure at infinity p_∞. The Bernoulli integral is

$$\frac{\partial\varphi}{\partial t}+\frac{1}{2}\left(\frac{\partial\varphi}{\partial r}\right)^2+h=0, \tag{2.3}$$

assuming that $\partial\varphi/\partial t\to 0$ at infinity. The kinematic condition at the bubble boundary $R(t)$ is

$$u(r,t)=\frac{\mathrm{d}R}{\mathrm{d}t}\quad\text{at } r=R(t), \tag{2.4}$$

while the condition on the normal stresses stipulates that

$$p_B(t)=p_{\mathrm{i}}(t)-\frac{1}{R}\left(2\sigma+4\mu\frac{\mathrm{d}R}{\mathrm{d}t}\right), \tag{2.5}$$

where p_B is the pressure on the liquid side of the interface, p_{i} the bubble internal pressure, σ the surface tension, and μ the viscosity. For the liquid we take a pressure–density relationship of the modified Tait form (Cole 1948)

$$\frac{p+B}{p_\infty+B}=\left(\frac{\rho}{\rho_\infty}\right)^n, \tag{2.6}$$

where B and n are constants and ρ_∞ denotes the undisturbed value of the density, from which we have the explicit expressions

$$c^2=\frac{n(p+B)}{\rho}=c_\infty^2+(n-1)h, \tag{2.7}$$

$$h=\frac{c^2-c_\infty^2}{n-1}=\frac{c_\infty^2}{n-1}\left[\left(\frac{p+B}{p_\infty+B}\right)^{(n-1)/n}-1\right]. \tag{2.8}$$

The boundary condition (2.5) will be enforced in the form

$$h(r,t)=h_B(t)\quad\text{at } r=R(t), \tag{2.9}$$

where h_B is obtained from (2.8) with p_B given by (2.5) and is

$$h_B(t) = \frac{n}{n-1}\frac{p_\infty + B}{\rho_\infty}\left[\left(\frac{p_i - \frac{2\sigma}{R} - \frac{4\mu}{R}\frac{\mathrm{d}R}{\mathrm{d}t} + B}{p_\infty + B}\right)^{(n-1)/n} - 1\right]. \tag{2.10}$$

3. Non-dimensional variables and scaling

We introduce scale units for length, R_0, and velocity, U, which will be taken of the order of the bubble size and bubble-wall velocity. The typical scales for time and enthalpy are T and H, respectively. In terms of these quantities the following non-dimensional variables, denoted by asterisks, are defined:

$$\left.\begin{aligned} r = R_0 r_*, \quad R = R_0 R_*, \quad t = T t_*, \\ \varphi = R_0 U \varphi_*, \quad h = H h_*, \quad c = c_\infty c_*. \end{aligned}\right\} \tag{3.1}$$

In the definition of φ_* we have taken $R_0 U$ as the appropriate scale for the potential in conformity with the relation $u = \partial\varphi/\partial r$. Upon substitution into (2.1), (2.3) and (2.4) it is found that three independent dimensionless parameters appear, which may be chosen as

$$C_1 = \frac{UT}{R_0}, \quad C_2 = \frac{H}{U^2}, \quad \epsilon = \frac{U}{c_\infty}. \tag{3.2}$$

In terms of the dimensionless quantities the equations become

$$\nabla_*^2 \varphi_* + \frac{\epsilon^2 C_2}{C_1}\frac{1}{c_*^2}\left(\frac{\partial h_*}{\partial t_*} + C_1 \frac{\partial \varphi_*}{\partial r_*}\frac{\partial h_*}{\partial r_*}\right) = 0, \tag{3.3}$$

$$\frac{\partial \varphi_*}{\partial t_*} + \tfrac{1}{2} C_1 \left(\frac{\partial \varphi_*}{\partial r_*}\right)^2 + C_1 C_2 h_* = 0, \tag{3.4}$$

$$C_1 \frac{\partial \varphi_*}{\partial r_*} = \frac{\mathrm{d}R_*}{\mathrm{d}t_*} \quad \text{at } r_* = R_*, \tag{3.5}$$

$$c_* = 1 + (n-1)\epsilon^2 C_2^2 h_*.$$

We shall consider this system in the limit

$$C_1 = O(1), \quad C_2 = O(1), \quad \epsilon \to 0. \tag{3.6}$$

The first condition stipulates that the bubble radius undergoes a change of order R_0 during the typical time T. It is dictated by the form of the boundary condition (3.5) if situations are to be described in which the velocity field in the liquid is influenced primarily by the motion of the bubble boundary. The enthalpy scale H is a measure of the internal energy of the liquid and $C_2 = O(1)$ implies that this energy is of the order of the kinetic energy, both per unit mass. This is clearly the situation of physical interest and is dictated by (3.4) if the dynamic boundary condition (2.9) is to play a significant role in the phenomenon investigated. Finally, ϵ is a measure of the Mach number of the liquid flow induced by the bubble-wall motion and the condition $\epsilon \ll 1$ is the appropriate one for the case of small compressibility effects.

In view of (3.6) we take $C_1 = C_2 = 1$. Furthermore, eliminating c_*^2 and h_* from (3.3)

using (2.7) and (2.8) we arrive at the following dimensionless equation for the potential:

$$\nabla_*^2\varphi_* = \epsilon^2\left\{\frac{\partial^2\varphi_*}{\partial t_*^2}+2\frac{\partial\varphi_*}{\partial r_*}\frac{\partial^2\varphi_*}{\partial r_*\partial t_*}+\left(\frac{\partial\varphi_*}{\partial r_*}\right)^2\frac{\partial^2\varphi_*}{\partial r_*^2}+(n-1)\left[\frac{\partial\varphi_*}{\partial t_*}+\frac{1}{2}\left(\frac{\partial\varphi_*}{\partial r_*}\right)^2\right]\nabla_*^2\varphi_*\right\}. \tag{3.7}$$

Equations (3.4), (3.5) and (2.9) are

$$\frac{\partial\varphi_*}{\partial t_*}+\frac{1}{2}\left(\frac{\partial\varphi_*}{\partial r_*}\right)^2+h_* = 0, \tag{3.8}$$

$$\frac{\partial\varphi_*}{\partial r_*} = \frac{\mathrm{d}R_*}{\mathrm{d}t_*} \quad \text{at } r_* = R_*, \tag{3.9}$$

$$h_* = h_{B*} \quad \text{at } r_* = R_*. \tag{3.10}$$

To lowest order in ϵ the field equation (3.7) is just Laplace's equation and therefore we do not expect any strong shock wave to be predicted by these equations near the bubble. The analysis of the outer equations given later shows that, with the present model, shock waves do not form in the far field either. Such highly nonlinear effects can only be brought out by the use of scalings other than (3.6). For example, near the point of minimum radius of a very violent collapse, the motion is characterized by a very short timescale and large pressures. This implies C_1 small and C_2 large. In order to balance terms in the Bernoulli integral (3.4) we must have $C_1C_2 = 1$, and the group ϵ^2C_2/C_1 of the field equation (3.3) becomes $\epsilon^2C_2^2$. The appropriate scaling for this situation would then clearly be $C_2 = 1/\epsilon$, $C_1 = \epsilon$, which would bring the system into the form

$$\nabla_*^2\varphi_*+\frac{1}{1+(n-1)h_*}\left(\frac{\partial h_*}{\partial t_*}+\epsilon\frac{\partial\varphi_*}{\partial r_*}\frac{\partial h_*}{\partial r_*}\right) = 0, \tag{3.11}$$

$$\frac{\partial\varphi_*}{\partial t_*}+h_*+\tfrac{1}{2}\epsilon\left(\frac{\partial\varphi_*}{\partial r_*}\right)^2 = 0, \tag{3.12}$$

$$\epsilon\frac{\partial\varphi_*}{\partial r_*} = \frac{\mathrm{d}R_*}{\mathrm{d}t_*} \quad \text{at } r_* = R_*. \tag{3.13}$$

The lowest-order equations arising from this system describe a nonlinear wave and will therefore most likely lead to a shock wave in the vicinity of the bubble.

Ideally, the solution procedure for a situation of violent collapse should therefore involve the introduction of a boundary layer in time in which the solution of the system (3.11)–(3.13) is matched to that of (3.7)–(3.9). It is doubtful that such a complex analytical approach would lead to a usable approximate equation for the radial motion and that it would be superior to a direct numerical solution of the exact equations (2.1)–(2.6). Furthermore, the strong instability of the spherical shape which would set in in these circumstances might turn the whole analysis into a rather sterile mathematical exercise.

The primary concern of the present study is to derive an equation of motion for the bubble radius incorporating in an approximate way the effects of liquid compressibility and simple enough to be of practical use. Hence we restrict ourselves to the scaling (3.6), and therefore our results will only be applicable to situations in which shock-wave formation in the liquid has a negligible effect on the dynamics of

the bubble. A vast number of problems in which bubbles are involved fall into this category and, even when shock waves are important, our results can be a useful first approximation. We partially exploit some of the information obtained from the second scaling mentioned by noting that, near the point of minimum radius, (3.12) indicates that the proper scale for h is not u^2, but $\partial\varphi/\partial t$. Thus h can be large where $\partial\varphi/\partial t$ is large, even though the Mach number may be small. This observation suggests that we should not try to approximate h in terms of the pressure, as in (3.1) of I (which would be legitimate at small Mach numbers) but rather that we deal with the enthalpy directly. Accordingly, we shall make use of the exact functional relation (2.10). It will be seen from the numerical results that this procedure does indeed lead to a better description of the process. As noted in I, the use of h is the reason for the good performance of the Gilmore equation previously noted by Hickling & Plesset (1964).

4. Solution strategy

The speed of sound in the undisturbed liquid c_∞ and the timescale T define a length $L = c_\infty T$ which characterizes the order of magnitude of distances at which the effects of a finite (rather than infinite) speed of sound are significant. Since $C_1 = 1$ we have

$$\frac{R_0}{L} = \frac{U}{c_\infty} = \epsilon. \tag{4.1}$$

The presence of two very different spatial scales suggests the application of a singular perturbation method to the present problem. This will be done rather formally following the matched asymptotic expansion method as set out by Lagerstrom & Casten (1972), since the simpler approach of I, although adequate to order 1 and ϵ, will be seen to fail at order ϵ^2.

The important feature of the singular perturbation method is to allow a clear assessment of the orders of magnitude of the terms appearing in the equations in the different regions of the liquid. This result is obtained by the introduction of a scaled variable (Lagerstrom & Casten 1972)

$$r_\eta = \eta(\epsilon)\, r_* \tag{4.2}$$

into the equations of the problem. Different choices of the magnitude of the gauge functions $\eta(\epsilon)$ give rise to different limit forms of the equations as $\epsilon \to 0$. Some of these limit equations contain others, while they themselves are not contained in any other. These particularly 'rich' equations are termed *distinguished equations* and they are the equations to be solved. To illustrate this procedure we carry it out in detail at the lowest order in ϵ in §5 and at the next order in Appendix A.

It is clear that only the asymptotic behavior of $\eta(\epsilon)$ as $\epsilon \to 0$ is significant in this procedure. Therefore equivalence classes are introduced such that η_1 and η_2 belong to the same class if $\eta_1 = O(\eta_2)$ as $\epsilon \to 0$. All the functions η such that $\eta = O(\bar{\eta})$ are collectively denoted by ord $\bar{\eta}$. A partial ordering can be established among different equivalence classes such that

$$\text{ord}\,\eta_1 < \text{ord}\,\eta_2$$

if $\eta_1 = o(\eta_2)$ as $\epsilon \to 0$.

In the following we shall apply the method of matched asymptotic expansions considering simultaneously both (3.7) and (3.8). At first sight this might appear unnecessary since the potential can be obtained by solving (3.7) with the boundary

condition (3.9), and (3.8) used afterwards to calculate h. This procedure will be seen to result in problems in the matching of the enthalpy fields in the liquid, although it leads to a correct form of the bubble equation of motion. The origin of this difficulty is that, due to the differential operators acting on φ_* in (3.8), a solution for φ_* accurate to a certain order in ϵ does not necessarily result in the same accuracy for h_*.

5. Order zero

The solution of the problem to order zero and order one does not differ from that given in I. We shall nonetheless develop it again using the present version of the method of matched asymptotic expansions both as a check of the rather heuristic derivation given in I and to illustrate the mathematical technique.

Upon introduction of the stretched variable $r_\eta = \eta(\epsilon) r_*$ into (3.7) and (3.8) we find

$$\eta^2\left\{1-\epsilon^2(n-1)\left[\frac{\partial\varphi_*}{\partial t_*}+\tfrac{1}{2}\eta^2\left(\frac{\partial\varphi_*}{\partial r_\eta}\right)^2\right]\right\}\nabla_\eta^2\varphi_* = \epsilon^2\left[\frac{\partial^2\varphi_*}{\partial t_*^2}+2\eta^2\frac{\partial\varphi_*}{\partial r_\eta}\frac{\partial^2\varphi_*}{\partial r_\eta\,\partial t_*}+\eta^4\left(\frac{\partial\varphi_*}{\partial r_\eta}\right)^2\frac{\partial^2\varphi_*}{\partial r_\eta^2}\right], \quad (5.1)$$

$$\frac{\partial\varphi_*}{\partial t_*}+\tfrac{1}{2}\eta^2\left(\frac{\partial\varphi_*}{\partial r_\eta}\right)^2+h_* = 0. \quad (5.2)$$

The limit form of these equations as $\epsilon\to 0$ for varying orders of magnitude of η are as follows:

$$\nabla_\eta^2\varphi_* = 0, \quad \frac{\partial\varphi_*}{\partial t_*}+\frac{1}{2}\left(\frac{\partial\varphi_*}{\partial r_\eta}\right)^2+h_* = 0, \quad \operatorname{ord}\eta = \operatorname{ord}1, \quad (5.3)$$

$$\nabla_\eta^2\varphi_* = 0, \quad \frac{\partial\varphi_*}{\partial t_*}+h_* = 0, \quad \operatorname{ord}\epsilon < \operatorname{ord}\eta < \operatorname{ord}1, \quad (5.4)$$

$$\nabla_\eta^2\varphi_*-\frac{\partial^2\varphi_*}{\partial t_*^2} = 0, \quad \frac{\partial\varphi_*}{\partial t_*}+h_* = 0, \quad \operatorname{ord}\eta = \operatorname{ord}\epsilon, \quad (5.5)$$

$$\frac{\partial^2\varphi_*}{\partial t_*^2} = 0, \quad \frac{\partial\varphi_*}{\partial t_*}+h_* = 0, \quad \operatorname{ord}\eta < \operatorname{ord}\epsilon. \quad (5.6)$$

It is clear that (5.4) are contained in (5.3), which we express by saying that (5.3) have the domain of validity (Lagerstrom & Casten 1972)

$$\mathscr{D}_1^{(0)} = \{\eta \mid \operatorname{ord}\epsilon < \operatorname{ord}\eta \leqslant \operatorname{ord}1\}. \quad (5.7)$$

Similarly (5.4) and (5.6) are contained in (5.5) which therefore is valid in the domain

$$\mathscr{D}_0^{(0)} = \{\eta \mid \operatorname{ord}\eta < \operatorname{ord}1\}. \quad (5.8)$$

Upon reverting to dimensional variables it is readily seen that (5.3) are the incompressible formulation, (3.5) of I, which is therefore seen to be appropriate in the region $r_* = O(1)$ or $r = O(R_0)$, i.e. near the bubble, as expected. This is the inner domain as expressed by the index i in (5.7) and r_* is seen to be the appropriate variable in this domain. Equations (5.5) coincide with the linearized formulation

(3.6) of I which is thus shown to be valid for $r_* = O(1/\epsilon)$, or $r = O(L)$, i.e. in the outer domain (index o in (5.8)) far from the bubble. An appropriate spatial variable in this domain (in the sense that it is of order 1 in it) is evidently, from (4.2),

$$\tilde{r} = \epsilon r_*. \tag{5.9}$$

It is clear that the domains (5.7) and (5.8) have a common part, the *domain of overlap* which is given by

$$\mathscr{D}^{(0)} = \{\eta \mid \operatorname{ord}\epsilon < \operatorname{ord}\eta < \operatorname{ord}1\}. \tag{5.10}$$

Since in this domain both systems (5.3) and (5.5) reduce to (5.4) their solutions must also reduce to each other as $\epsilon \to 0$. This is the principle of matching that will supply (5.3) with an effective boundary condition at infinity and (5.5) with one near the bubble boundary.

We shall indicate the solution of the inner equations (5.3) by φ_0, h_0 since these quantities are the zero-order terms in the perturbation series to be constructed. These terms are readily found to be

$$\varphi_0(r_*, t_*) = -\frac{f_0(t_*)}{r_*} + g_0(t_*), \tag{5.11a}$$

$$h_0(r_*, t_*) = \frac{f_0'}{r_*} - g_0' - \frac{1}{2}\frac{f_0^2}{r_*^4}, \tag{5.11b}$$

where here and in the following the prime indicates differentiation with respect to the argument. The solution to (5.5), which will be indicated by ϕ_0, H_0 and expressed in terms of the outer variable $\tilde{r}$ defined by (5.9), is

$$\phi_0(\tilde{r}, t_*) = \frac{1}{\tilde{r}}[F_0(t_* - \tilde{r}) + G_0(t_* + \tilde{r})] + \alpha_0, \tag{5.12a}$$

$$H_0(\tilde{r}, t_*) = -\frac{1}{\tilde{r}}[F_0'(t_* - \tilde{r}) + G_0'(t_* + \tilde{r})], \tag{5.12b}$$

where α_0 is an integration constant. The matching of the two solutions is expressed formally by

$$\lim_{\epsilon \to 0}\left[\varphi_0\left(\frac{r_\eta}{\eta}, t_*\right) - \phi_0\left(\frac{\epsilon}{\eta} r_\eta, t_*\right)\right] - 0, \tag{5.13}$$

for fixed r_η and for any function $\eta(\epsilon)$ belonging to the overlap domain (5.10). A similar relation must be satisfied by h_0 and H_0. Upon substitution of (5.11*a*), (5.12*a*) into (5.13) it is readily found that this condition is satisfied if and only if

$$F_0 = -G_0, \quad g_0(t_*) = 2G_0'(t_*) + \alpha_0. \tag{5.14}$$

The enthalpy fields also match if these two relations hold. The solution thus determined coincides with that given in §5 of I. The kinematic boundary condition (3.9) gives

$$f_0 = R_*^2 R_*', \tag{5.15}$$

and the dynamic one (3.10)

$$\frac{(R_*^2 R_*')'}{R_*} - \tfrac{1}{2}R_*'^2 = 2G_0'' + h_{B*} + O(\epsilon) \tag{5.16}$$

or

$$R_* R_*'' + \tfrac{3}{2}R_*'^2 = 2G_0'' + h_{B*}, \tag{5.17}$$

where h_{B*} is given by (2.10) after non-dimensionalization. This is the Rayleigh–Plesset equation written in terms of the enthalpy rather than the pressure as is more customary (see the comments in I).

6. First order

In order to proceed with the perturbation scheme we set

$$\varphi_* = \varphi_0 + \epsilon\varphi_1, \quad h_* = h_0 + \epsilon h_1, \tag{6.1}$$

where φ_0, h_0 are given by (5.11) and satisfy (5.3) and where φ_1, h_1 are, for the time being, such that the exact solution is obtained. In other words, φ_1 is defined by $\varphi_1 = (\varphi_* - \varphi_0)/\epsilon$, where φ_* is the exact solution, and similarly for h_1. Upon substitution of (6.1) into (3.7) and use of (5.3) one finds a complicated equation for φ_1 which is given in full in Appendix A. This equation, which is still exact, is now to be solved approximately by the same method used at the previous order. Thus, we study its formal limits under the scaling (4.2) of the spatial variable and single out the distinguished equations. In this process it should be kept in mind that one can expect φ_1 to be of order 1 only in the domain where φ_0 is a 'good' approximation (i.e. to order 1) of the solution of the original problem. Hence, only scalings belonging to the inner domain (5.7) should be considered. The same procedure is then carried out on the equation for h_1 which is obtained by substituting (6.1) into (3.8). Further details on the method are outlined in Appendix A. Here we proceed directly with the results.

Unlike the situation at the previous order, one finds two distinct distinguished limits, both arising from the inner domain. The first one occurs for $\eta = O(1)$ and is

$$\nabla_*^2 \varphi_1 = 0, \tag{6.2a}$$

$$h_1 = -\frac{\partial \varphi_1}{\partial t_*} - \frac{\partial \varphi_0}{\partial r_*}\frac{\partial \varphi_1}{\partial r_*}. \tag{6.2b}$$

The second one occurs for $\eta = O(\epsilon^{\frac{1}{2}})$ and is

$$\bar{\nabla}^2 \varphi_1 = 2G_0'''(t_*), \quad h_1 = -\frac{\partial \varphi_1}{\partial t_*}, \tag{6.3a, b}$$

where the Laplacian is with respect to the variable

$$\bar{r} = \epsilon^{\frac{1}{2}} r_*. \tag{6.4}$$

The domain of validity of (6.2) is found to be

$$\mathscr{D}_1^{(1)} = \{\eta \mid \operatorname{ord} \epsilon^{\frac{1}{2}} < \operatorname{ord} \eta \leqslant \operatorname{ord} 1\}, \tag{6.5}$$

while, for (6.3)

$$\overline{\mathscr{D}_1^{(1)}} = \{\eta \mid \operatorname{ord} \epsilon < \operatorname{ord} \eta < \operatorname{ord} 1\}. \tag{6.6}$$

It may be noted that both domains are contained in the domain of validity (5.7) of the zero-order inner approximation and that they overlap in $\operatorname{ord} \epsilon^{\frac{1}{2}} < \operatorname{ord} \eta < \operatorname{ord} 1$.

In a similar way, to obtain the next term in the outer expansion, we set

$$\varphi_* = \phi_0 + \epsilon\phi_1, \quad h_* = H_0 + \epsilon H_1, \tag{6.7}$$

with ϕ_0, H_0 the solutions (5.12) of (5.5) and ϕ_1, H_1 exact. When the full equations for ϕ_1 and H_1, given in Appendix A, are analysed under the scaling (4.2), only one distinguished limit results, namely

$$\tilde{\nabla}\phi_1 - \frac{\partial^2 \phi_1}{\partial t_*^2} = 0, \quad \frac{\partial \phi_1}{\partial t_*} + H_1 = 0. \tag{6.8a, b}$$

This limit is obtained for ord η = ord ϵ and has a formal domain of validity ord $\eta \leqslant$ ord 1 which must, however, be restricted to (5.8) if ϕ_1, H_1 are to be guaranteed to be of order 1, as already explained. Equations (6.8) are the same as (5.5).

The domain of validity of the 'outer inner' equations (6.3) is contained in that of the outer equations (6.8) which suggests that (6.3) need not be considered. Indeed it is found that matching the solution of (6.2) with that of (6.3), and the latter with that of (6.8) leads, to a consistent order, to the same result as matching the solution of (6.2) and (6.8) directly in their domain of overlap

$$\mathscr{D} = \{\eta \mid \text{ord}\, \epsilon^{\frac{1}{3}} < \text{ord}\, \eta < \text{ord}\, 1\}. \tag{6.9}$$

It may be noted that this domain is smaller than the domain of overlap (5.10) of the zero-order solution.

The solution of (6.2a) is the same as (5.11a) with $f_0(t_*)$, $g_0(t_*)$ replaced by $f_1(t_*)$, $g_1(t_*)$. The kinematic boundary condition (3.9) leads however to $f_1 = 0$ and therefore

$$\varphi_1(r_*, t_*) = g_1(t_*), \quad h_1(r_*, t_*) = -g_1'(t_*). \tag{6.10a,b}$$

Similarly, the solution of (6.8) has the same form as (5.12) with F_0, G_0 replaced by $F_1(t_* - \tilde{r})$, $G_1(t_* + \tilde{r})$.

The solutions found for (φ_1, h_1), (ϕ_1, H_1) differ, in their respective domains, from the exact ones by terms $o(1)$ and therefore the error in using them in (6.1) and (6.7) is $o(\epsilon)$. Hence the matching condition (5.13) must now take the form

$$\lim_{\epsilon \to 0} \frac{1}{\epsilon}\left[(\varphi_0 + \epsilon\varphi_1)\left(\frac{r_\eta}{\eta}, t_*\right) - (\phi_0 + \epsilon\phi_1)\left(\frac{\epsilon}{\eta} r_\eta, t_*\right)\right] = 0, \tag{6.11}$$

for η in the domain (6.9) and r_η fixed. This condition leads to

$$F_1 = -f_0 - G_1, \quad g_1 = 2G_1' + f_0'. \tag{6.12a,b}$$

When the same condition (6.11) is applied to the enthalpy fields it is found that matching occurs if (6.12) are satisfied, not in the entire domain (6.9) but only in the smaller one

$$\mathscr{D}^{(1)} = \{\eta \mid \text{ord}\, \epsilon^{\frac{1}{3}} < \text{ord}\, \eta < \text{ord}\, \epsilon^{\frac{1}{4}}\}. \tag{6.13}$$

The restriction to ord $\eta <$ ord $\epsilon^{\frac{1}{4}}$ is made necessary by the term r_*^{-4} in h_0 which cannot be balanced by any term in $H_0 + \epsilon H_1$ and must therefore disappear in the limit $\epsilon \to 0$. This rapid shrinking of the domains of overlap of the inner and outer solutions suggests that intermediate solutions may be required at higher orders and indeed this will be found to be the case at the next order.

With (6.12) the outer potential becomes, at this order

$$\phi_0 + \epsilon\phi_1 = \frac{1}{\tilde{r}}[G_0(t_* + \tilde{r}) - G_0(t_* - \tilde{r})] + \alpha_0 + \frac{\epsilon}{\tilde{r}}[G_1(t_* + \tilde{r}) - G_1(t_* - \tilde{r}) - f_0(t_* - \tilde{r})]. \tag{6.14}$$

The terms in ϵ represent the effect of the perturbation (i.e. the bubble) on the potential far away. It is obvious that in the absence of boundaries the bubble cannot affect the incoming pressure perturbation which leads one to set $G_1 = 0$. Recalling

that $f_0 = R_*^2 R_*'$, we can now write the final form of the potential and enthalpy fields valid to order ϵ. In the near field we have

$$\varphi_0 + \epsilon\varphi_1 = -\frac{R_*^2 R_*'}{r_*} + 2G_0'(t_*) + \alpha_0 + \epsilon(R_*^2 R_*')', \tag{6.15a}$$

$$h_0 + \epsilon h_1 = \frac{(R_*^2 R_*')'}{r_*} - \frac{1}{2}\frac{(R_*^2 R_*')^2}{r_*^4} - 2G_0''(t_*) - \epsilon(R_*^2 R_*')''(t_*); \tag{6.15b}$$

while in the far field

$$\phi_0 + \epsilon\phi_1 = \frac{1}{\tilde{r}}[G_0(t_* + \tilde{r}) - G_0(t_* - \tilde{r})] - \frac{\epsilon}{\tilde{r}}(R_*^2 R_*')(t_* - \tilde{r}) + \alpha_0, \tag{6.16a}$$

$$H_0 + \epsilon H_1 = -\frac{1}{\tilde{r}}[G_0'(t_* + \tilde{r}) - G_0'(t_* - \tilde{r})] + \frac{\epsilon}{\tilde{r}}(R_*^2 R_*')'(t_* - \tilde{r}). \tag{6.16b}$$

The effect of the bubble appears in the far field as that of a standard acoustic monopole evaluated at the retarded time $t_* - \tilde{r}$ or, in dimensional variables, $t - r/c_\infty$. The bubble also gives a small contribution to the space-independent part of the near-field enthalpy and potential, which are otherwise unaltered from the previous order. These expressions agree with those derived more heuristically in §5 of I.

With the result (6.15*b*) for the enthalpy field in the liquid we can now impose the second boundary condition (3.10) that the enthalpy on the liquid side of the interface equal h_{B*} to find

$$\frac{(R_*^2 R_*')'}{R_*} - \tfrac{1}{2}R_*'^2 - 2G_0''(t_*) - \epsilon(R_*^2 R_*')''(t_*) = h_{B*} + O(\epsilon^2). \tag{6.17}$$

If the indicated differentiation in the last term in the left-hand side is carried out a term containing R_*''' appears. To avoid this we note that, since the error in (6.17) is of order ϵ^2, it is sufficient to approximate this term correctly to order 1. For this purpose we differentiate the dimensionless Rayleigh–Plesset equation in the form (5.16) and use the result to eliminate $(R_*^2 R_*')''$ to find

$$(1 - \epsilon R_*') R_* R_*'' + \tfrac{3}{2}(1 - \tfrac{1}{3}\epsilon R_*') R_*'^2 = (1 + \epsilon R_*')(h_{B*} + 2G_0'') + \epsilon R_* \frac{\mathrm{d}}{\mathrm{d}t_*}(h_{B*} + 2G_0'') + O(\epsilon^2). \tag{6.18}$$

This is the dimensionless form of the equation derived by Keller and co-workers (Keller & Kolodner 1956; Epstein & Keller 1971; Keller & Miksis 1980). However this form is not unique, as shown in I. If (5.17) is multiplied by $\epsilon\lambda R_*'$, where λ is a numerical constant of order 1 (or, at any rate, of smaller order than $1/\epsilon$), and subtracted from (6.18) one finds

$$[1 - (\lambda + 1)\epsilon R_*'] R_* R_*'' + \tfrac{3}{2}[1 - (\lambda + \tfrac{1}{3})\epsilon R_*'] R_*'^2 = [1 + (1 - \lambda)\epsilon R_*'](h_{B*} + 2G_0'') + \epsilon R \frac{\mathrm{d}}{\mathrm{d}t_*}(h_{B*} + 2G_0''), \tag{6.19}$$

which evidently has the same accuracy as (6.18). In particular, for $\lambda = 1$, the form given by Herring (1941; see also Trilling 1952) is found. In I (6.19) has been called the general Keller–Herring equation.

7. Second order

As in §6 we set, in the inner field,

$$\varphi_* = \varphi_0 + \epsilon\varphi_1 + \epsilon^2\varphi_2, \quad h_* = h_0 + \epsilon h_1 + \epsilon^2 h_2, \tag{7.1}$$

where (φ_0, h_0) are the solutions of (5.3), (φ_1, h_1) are the solutions of (6.2), while (φ_2, h_2) are, at this point, exact. Upon substitution into the original equations (3.7) and (3.8) a complicated set of equations is obtained which we shall not reproduce for brevity. When an analysis of the formal limits parallel to that done for the zero-order case in §5 is carried out, it is found that only one distinguished limit exists, namely

$$\nabla_*^2\varphi_2 = 2G_0''' - \frac{f_0''}{r_*} + \frac{2f_0f_0'}{r_*^4} - \frac{2f_0^3}{r_*^7}, \tag{7.2a}$$

$$\frac{\partial\varphi_2}{\partial t_*} + \frac{f_0}{r_*^2}\frac{\partial\varphi_2}{\partial r_*} + h_2 = 0, \tag{7.2b}$$

where the argument of G_0 and f_0 is t_*. The domain of validity of these equations coincides with that of the inner equations of the previous order (6.5).

In the same way, upon setting

$$\varphi_* = \phi_0 + \epsilon\phi_1 + \epsilon^2\phi_2, \quad h_* = H_0 + \epsilon H_1 + \epsilon^2 H_2, \tag{7.3}$$

in (3.7) and (3.8) and taking into account (5.5) and (6.1) one finds an equation set which possesses two distinguished limits. The first one occurs for ord η = ord $\epsilon^{\frac{1}{2}}$. In terms of the scaled variable $\bar{r}$ defined in (6.4) the corresponding equations are

$$\bar{\nabla}^2\phi_2 = 0, \tag{7.4}$$

$$\frac{\partial\phi_2}{\partial t_*} + \tfrac{1}{2}\frac{f_0^2(t_*)}{\bar{r}^4} + H_2 = 0, \tag{7.5}$$

with a domain of validity

$$\mathscr{D} = \{\eta \mid \text{ord}\,\epsilon < \text{ord}\,\eta < \text{ord}\,\epsilon^{\frac{1}{2}}\}. \tag{7.6}$$

Formally the upper bound is found to be ord 1 rather than ord $\epsilon^{\frac{1}{2}}$, but the restriction is required by consistency with (6.13). The second set of distinguished-limit equations is

$$\tilde{\nabla}^2\phi_2 - \frac{\partial^2\phi_2}{\partial t_*^2} = \frac{1}{\tilde{r}}\Gamma(\tilde{r}, t_*), \tag{7.7a}$$

$$\frac{\partial\phi_2}{\partial t_*} + H_2 = -\frac{1}{2}\frac{1}{\tilde{r}^2}[G_+' + G_-' - \frac{1}{\tilde{r}}(G_+ - G_-)]^2, \tag{7.7b}$$

where

$$\Gamma(\tilde{r}, t_*) = \frac{2}{\tilde{r}}(G_+' + G_-')(G_+'' + G_+'') + \frac{n-1}{\tilde{r}}(G_+' - G_-')(G_+'' - G_-'')$$

$$-\frac{2}{\tilde{r}^2}[(G_+ - G_-)(G_+'' + G_-'') + G_+'^2 - G_-'^2] + \frac{2}{\tilde{r}^3}(G_+ - G_-)(G_+' - G_-'), \tag{7.8}$$

$$G_\pm = G_0(t_* \pm \tilde{r}), \tag{7.9}$$

with the prime indicating differentiation with respect to the argument. Note that in the case of free motion $\Gamma = 0$. The domain of validity of (7.7) is

$$\mathscr{D}_0^{(2)} = \{\eta \mid \text{ord}\,\eta < \text{ord}\,\epsilon^{\frac{1}{2}}\}, \tag{7.10}$$

which overlaps with that of (7.4), (7.5) in

$$\mathscr{D}'^{(2)} = \{\eta \mid \operatorname{ord}\epsilon < \operatorname{ord}\eta < \operatorname{ord}\epsilon^{\frac{1}{2}}\}. \tag{7.11}$$

The domain of validity of the inner equations (7.2) overlaps with that of the intermediate equations (7.4), (7.5) in

$$\mathscr{D}^{(2)} = \{\eta \mid \operatorname{ord}\epsilon^{\frac{1}{2}} < \operatorname{ord}\eta < \operatorname{ord}\epsilon^{\frac{1}{2}}\}. \tag{7.12}$$

These two domains are evidently disjoint, which shows that (7.4), (7.5) are essential in the mathematical structure of the problem, unlike (6.3) of the previous order.

The solution of (7.4), (7.5) is

$$\bar{\phi}_2 = -\frac{\bar{f}_2(t_*)}{\bar{r}} + \bar{g}_2(t_*), \tag{7.13a}$$

$$\bar{H}_2 = -\bar{g}_2'(t_*) + \frac{\bar{f}_2'(t_*)}{\bar{r}} - \frac{1}{2}\frac{f_0^2(t_*)}{\bar{r}^4}, \tag{7.13b}$$

where an overbar has been introduced to distinguish these functions from the solution of (7.7) which is found to be

$$\tilde{\phi}_2 = \frac{1}{\tilde{r}}[F_2(t-\tilde{r}) - \psi], \tag{7.14a}$$

$$\tilde{H}_2 = -\frac{1}{\tilde{r}}\left[F_2'(t-\tilde{r}) - \frac{\partial\psi}{\partial t_*}\right] - \tfrac{1}{2}\frac{1}{\tilde{r}^2}\left[G_+' + G_-' - \frac{1}{\tilde{r}}(G_+ - G_-)\right]^2, \tag{7.14b}$$

where, as shown in Appendix B,

$$\psi(\tilde{r}, t_*) = \frac{1}{2}\int_0^{t_*} \mathrm{d}\tau \int_\tau^{t_*} [\Gamma(\tilde{r}+\theta-\tau, \tau) + \Gamma(\tilde{r}-\theta+\tau, \tau)]\,\mathrm{d}\theta. \tag{7.15}$$

We proceed now to match (7.13) with (7.14). It should be noted that $(\bar{\phi}_2, \bar{H}_2)$ and $(\tilde{\phi}_2, \tilde{H}_2)$ are to be considered as lowest-order approximations to (ϕ_2, H_2) defined in (7.3) valid in different domains. Hence these solutions should match with a difference of $o(1)$, i.e.

$$\lim_{\epsilon\to 0}\left[\tilde{\phi}_2\left(\frac{\epsilon}{\eta}r_\eta, t_*\right) - \bar{\phi}_2\left(\frac{\epsilon^{\frac{1}{2}}}{\eta}r_\eta, t_*\right)\right] = 0, \tag{7.16}$$

for η in the domain (7.11). In imposing this condition it is useful to note that, since $\psi(0, t_*) = 0$, for $\tilde{r}$ small one has approximately

$$\psi(\tilde{r}, t_*) \approx \tilde{r}\int_0^{t_*} \Gamma(t_*-\tau, \tau)\,\mathrm{d}\tau + O(\tilde{r}^2). \tag{7.17}$$

The result of (7.16) is then

$$\bar{g}_2(t_*) = -\int_0^{t_*} \Gamma(t_*-\tau, \tau)\,\mathrm{d}\tau, \quad F_2 = 0. \tag{7.18}$$

Rather than carrying both (7.13) and (7.14) it is more convenient to combine them in a composite expansion as follows:

$$\phi_2 = -\frac{\psi(\tilde{r}, t_*)}{\tilde{r}} - \frac{1}{\tilde{r}}\bar{f}_2(t_*),$$

$$H_2 = \frac{1}{\tilde{r}}\frac{\partial\psi}{\partial t_*} - \frac{1}{2}\left(\frac{\partial\varphi_0}{\partial\tilde{r}}\right)^2 + \frac{\bar{f}_2'}{\bar{r}} - \frac{1}{2}\frac{f_0^2}{\bar{r}^4}.$$

It is readily verified that, for η in the outer domain (7.10), $(\phi_2, H_2) \to (\tilde{\phi}_2, \tilde{H}_2)$, while for η in the overlap domain (7.11), $(\phi_2, H_2) \to (\bar{\phi}_2, \bar{H}_2)$.

The solution of the inner equations (7.2) is

$$\varphi_2 = \tfrac{1}{3}G_0''' r_*^2 - \tfrac{1}{2}f_0'' r_* + \frac{f_0 f_0'}{r_*^2} - \frac{f_0^3}{10 r_*^5} - \frac{f_2}{r_*} + g_2, \tag{7.19a}$$

$$h_2 = -\tfrac{1}{3}G_0^{\mathrm{iv}} r_*^2 + \tfrac{1}{2}f_0''' r_* - g_2' + (f_2' - \tfrac{2}{3}G_0''' f_0)\frac{1}{r_*} - (\tfrac{1}{2}f_0'' f_0 + f_0'^2)\frac{1}{r_*^2} + \frac{23}{10}\frac{f_0^2 f_0'}{r_*^5} - \frac{1}{2}\frac{f_0^4}{r_*^8} - \frac{f_2 f_0}{r_*^4}. \tag{7.19b}$$

The kinematic boundary condition (3.9) requires that $\partial\varphi_2/\partial r_* = 0$ at $r_* = R_*$ and leads to

$$f_2 = -\tfrac{2}{3}G_0''' R_*^3 + \tfrac{1}{2}f_0''' R_*^2 + 2\frac{f_0 f_0'}{R_*} - \frac{1}{2}\frac{f_0^3}{R_*^4}. \tag{7.20}$$

The solution (7.19) must now be matched with the intermediate one (7.13). By an argument similar to that leading to (6.11) the appropriate condition has the form

$$\lim_{\epsilon\to 0}\frac{1}{\epsilon^2}\left\{(\varphi_0 + \epsilon\varphi_1 + \epsilon^2\varphi_2)\left(\frac{r_\eta}{\eta}, t_*\right) - \left[(\phi_0 + \epsilon\phi_1)\left(\frac{\epsilon}{\eta}r_\eta, t_*\right) + \epsilon^2\bar{\phi}_2\left(\frac{\epsilon^{\frac{1}{2}}}{\eta}r_\eta, t_*\right)\right]\right\} = 0, \tag{7.21}$$

and similarly for the enthalpy, and results in

$$\bar{f}_2 = 0, \quad g_2 = \bar{g}_2 = -\int_0^{t_*} \Gamma(t_* - \tau, \tau)\,\mathrm{d}\tau. \tag{7.22}$$

It may be noted that, if the necessity of an intermediate solution had not been realized, these same conditions would have been found by matching the inner potential (7.19*a*) directly with the 'outer outer' one (7.14*a*). The inner enthalpy would have been determined exactly in this way and, since the radial equation of motion depends only on this inner field, the proper equation would have been found even though the enthalpy fields do not match without the intermediate field (7.13*b*). This procedure would therefore have resulted in a correct equation of motion, but an erroneous enthalpy distribution in the liquid.

We are now in a position to obtain the second-order-accurate equation for the radius.

8. Second-order equations for the radius

The dynamical boundary condition at the bubble wall is to be imposed in the form

$$(h_0 + \epsilon h_1 + \epsilon^2 h_2)(r_* = R_*, t_*) = h_{B*}(t_*). \tag{8.1}$$

Using the preceding results (6.15*b*), (7.19*b*) we find, after some reduction,

$$R_* R_*'' + \tfrac{3}{2}R_*'^2 - 2G_0'' - \epsilon(R_*^2 R_*')'' + \epsilon^2[(R_*^2 R_*')''' R_* + 2(R_*^2 R_*')'' R_* - \tfrac{2}{5}R_*'^4 + \tfrac{4}{5}R_* R_*'^2 R_*'' + R_*^2 R_*''^2 - 2G_0''' R_* R_* - G_0^{\mathrm{iv}} R_*^2 - g_2'] = h_{B*} + O(\epsilon^2), \tag{8.2}$$

where all the quantities have argument t_*, and g_2 is given by the second of (7.22). As before we encounter the problem that, upon expansion of the indicated derivatives, derivatives of R_* up to the fourth order appear. However, since these higher derivatives are multiplied by ϵ and ϵ^2, the previous, less accurate results can be used

for their evaluation. In particular, upon differentiation of the first-order equation (6.17), one finds

$$\epsilon(R_*^2 R_*')''' = \frac{(R_*^2 R_*')''}{R_*} - \frac{(R_*^2 R_*')'}{R_*^2} R_*' - R_*' R_*'' - \frac{\mathrm{d}}{\mathrm{d}t}(h_{B*} + 2G_0'') + O(\epsilon^2), \tag{8.3}$$

which can be used to express the first term in the square brackets in (8.2) with the result

$$\begin{aligned} R_* R_*'' + \tfrac{3}{2} R_*'^2 - 2\epsilon R_*'(R_*'^2 + R_* R_*'') - \epsilon R_* \frac{\mathrm{d}}{\mathrm{d}t}(h_{B*} + 2G_0'') + \epsilon^2 [2R_*'(R_*^2 R_*')'' \\ - \tfrac{2}{5} R_*'^4 + \tfrac{4}{5} R_* R_*'^2 R_*'' + R_*^2 R_*''^2 - 2G_0''' R_* R_*' - G_0^{\mathrm{iv}} R_*^2 - g_2'] \\ = h_{B*} + 2G_0'' + O(\epsilon^2). \end{aligned} \tag{8.4}$$

The last step is to eliminate $(R_*^2 R_*')''$. This can be done with an accuracy of order one, and hence use can be made of the Rayleigh–Plesset equation (5.16) to find

$$(R_*^2 R_*')'' = R_*'(\tfrac{1}{2} R_*'^2 + 2G_0'' + h_{B*}) + R_* \left[R_*' R_*'' + \frac{\mathrm{d}}{\mathrm{d}t}(2G_0'' + h_{B*}) \right]. \tag{8.5}$$

The final result is

$$\begin{aligned} (1 - 2\epsilon R_*' + \tfrac{14}{5} \epsilon^2 R_*'^2) R_* R_*'' + \tfrac{3}{2}(1 - \tfrac{4}{3}\epsilon R_*' + \tfrac{2}{5}\epsilon^2 R_*'^2) R_*'^2 + \epsilon^2 R_*^2 R_*''^2 \\ = (1 - 2\epsilon^2 R_*'^2)(h_{B*} + 2G_0'') + \epsilon(1 - 2\epsilon R_*') R_* \frac{\mathrm{d}}{\mathrm{d}t_*}(h_{B*} + 2G_0'') \\ + \epsilon^2 [2G_0''' R_* R_*' + G_0^{\mathrm{iv}} R_*^2 + g_2'] + O(\epsilon^3). \end{aligned} \tag{8.6}$$

The non-uniqueness found at the previous step acquires now an extra degree of freedom. Indeed, by multiplying the Keller equation (6.18) by $(1-\lambda)\epsilon R_*'$ and the Rayleigh–Plesset equation (5.17) by $(\theta + \lambda + 1)\epsilon^2 R_*'^2$, where again λ and θ are numerical constants of order 1, and adding to (8.6) we find

$$\begin{aligned} [1 - (\lambda+1)\epsilon R_*' + (\tfrac{14}{5} + 2\lambda + \theta)\epsilon^2 R_*'^2] R_* R_*'' \\ + \tfrac{3}{2}[1 - (\lambda + \tfrac{1}{3})\epsilon R_*' + (\tfrac{16}{15} + \tfrac{4}{3}\lambda + \theta)\epsilon^2 R_*'^2] R_*'^2 + \epsilon^2 R_*^2 R_*''^2 \\ = [1 + (1-\lambda)\epsilon R' + \theta\epsilon^2 R_*'^2](h_{B*} + 2G_0'') \\ + \epsilon[1 - (1+\lambda)\epsilon R_*'] R_* \frac{\mathrm{d}}{\mathrm{d}t_*}(h_{B*} + 2G_0'') \\ + \epsilon^2 [2G_0''' R_* R_*' + G_0^{\mathrm{iv}} R_*^2 + g_2'] + O(\epsilon^3), \end{aligned} \tag{8.7}$$

which evidently has the same degree of accuracy as (8.6).

Still other variants of this equation are possible. For example, using the Rayleigh–Plesset equation (5.17) to express $R_* R_*''$, we may write

$$\epsilon^2 R_*^2 R_*''^2 = \epsilon^2 R_* R_*''(2G_0'' + h_{B*} - \tfrac{3}{2} R_*'^2) + O(\epsilon^3), \tag{8.8a}$$

or, alternatively,

$$\epsilon^2 R_*^2 R_*''^2 = \epsilon^2 (2G_0'' + h_{B*} - \tfrac{3}{2} R_*'^2)^2 + O(\epsilon^3). \tag{8.8b}$$

In the first case (8.7) becomes

$$\begin{aligned}&[1-(\lambda+1)\,\epsilon R'_*+\epsilon^2(2G''_0+h_{B*})+\epsilon^2(\tfrac{13}{10}+2\lambda+\theta)\,R'^2_*]\,R_*\,R''_*\\&\quad+\tfrac{3}{2}[1-(\lambda+\tfrac{1}{3})\,\epsilon R'_*+(\tfrac{16}{15}+\tfrac{4}{3}\lambda+\theta)\,\epsilon^2 R'^2_*]\,R'^2_*\\&=[1+(1-\lambda)\,\epsilon R'_*+\epsilon^2\theta R'^2_*]\,(h_{B*}+2G''_0)\\&\quad+\epsilon[1-(1+\lambda)\,\epsilon R'_*]\,R_*\frac{\mathrm{d}}{\mathrm{d}t_*}(h_{B*}+2G''_0)\\&\quad+\epsilon^2[2G'''_0\,R_*\,R'_*+G^{\mathrm{iv}}_0\,R^2_*+g'_2]+O(\epsilon^3).\end{aligned}\tag{8.9}$$

A corresponding family of equations may be obtained by approximating the enthalpy h_{B*} as in (3.1) of I,

$$h_{B*}=p_{B*}-\tfrac{1}{2}\epsilon^2 p^2_{B*}+O(\epsilon^4),\tag{8.10}$$

where

$$p_{B*}=\frac{p_B-p_\infty}{\rho_\infty U^2},\tag{8.11}$$

with p_B given by (2.5). The corresponding form of the Rayleigh–Plesset equation (5.17),

$$R_*\,R''_*+\tfrac{3}{2}R'^2_*=2G''_0+p_{B*}+O(\epsilon),\tag{8.12}$$

can then be used to eliminate the term $(\epsilon R_*\,R''_*)^2$ as in (8.8*b*). For free motion (i.e. with $G_0=0$, $g_2=0$), with the choice $\lambda=1$, $\theta=0$, the resulting equation is

$$\begin{aligned}&(1-2\,\epsilon R'_*+\tfrac{23}{10}\epsilon^2 R'^2_*)\,R_*\,R''_*+\tfrac{3}{2}(1-\tfrac{4}{3}\epsilon R'_*+\tfrac{7}{5}\epsilon^2 R'^2_*)\,R'^2_*\\&\qquad=p_{B*}+\epsilon R_*(1-2\epsilon R'_*)\frac{\mathrm{d}p_{B*}}{\mathrm{d}t_*}-\tfrac{1}{2}\epsilon^2 p_{B*}(3p_{B*}-R'^2_*)+O(\epsilon^3).\end{aligned}\tag{8.13}$$

This is the non-dimensional form of the equation derived by Tomita & Shima (1977; see also Fujikawa & Akamatsu 1980). Although this equation has the same order of accuracy as all the others, it possesses the spurious equilibrium solution

$$p_{B*}=\frac{3}{2\epsilon^2}.\tag{8.14}$$

This large value of p_{B*} is evidently outside the range where the perturbation procedure can be expected to be accurate, but its formal existence may cause difficulties in numerical integration.

While observations such as the one just made may indicate that some equations are less suitable than others, it is clear that no *a priori* criteria exist for the selection of one particular form. Furthermore, examination of (8.7) does not give any indication about a possible optimal choice of the parameter λ for the first-order equation (6.19). We shall examine the performance of (8.7) and (8.9) by comparison with the numerical solution of the original partial-differential-equation formulation in §10. In §11 other equations available in the literature will be examined in the light of our results.

It may be of some interest to note as a final point that, in the case of forced motion, all the second-order equations contain the term $g'_2(t_*)$ which, as is clear from the definition (7.18), depends on the past history of the incoming pressure field.

9. Composite expansions for the fields

In the preceding sections the solution for the enthalpy and potential has been obtained in the form of expansions valid in different regions of the liquid. We propose here to combine these results deriving single expressions uniformly valid to orders 1 and ϵ throughout the liquid, the so-called *composite expansions*. The most direct approach to this task runs into a difficulty which will be illustrated in its simplest form for the order-1 case. From (5.11) and (5.12) it is clear by inspection that

$$\varphi_*^{(0)} = \frac{1}{\epsilon r_*}[G_0(t_*+\epsilon r_*)-G_0(t_*-\epsilon r_*)]-\frac{(R_*^2 R'_*)(t_*)}{r_*}+\alpha_0, \tag{9.1a}$$

$$h_*^{(0)} = -\frac{1}{\epsilon r_*}[G'_0(t_*+\epsilon r_*)-G'_0(t_*-\epsilon r_*)]+\frac{(R_*^2 R'_*)'(t_*)}{r_*}-\frac{1}{2}\frac{R_*^4(t_*)}{r_*^4}R'_*(t_*), \tag{9.1b}$$

reduce to the appropriate forms in the inner and outer domains with errors of order $o(1)$, i.e. consistent with the degree of accuracy of (5.11) and (5.12) themselves. While expressions such as (9.1) and their higher-order analogues are formally valid throughout the liquid, their use runs into practical difficulties as they satisfy the boundary conditions at the bubble boundary only in the limit $\epsilon \to 0$, and not for ϵ small but finite. The problem can be illustrated by considering the velocity field obtained from the first-order analogue of (9.1a), which is shown by the dashed line in figure 1. In this figure the bubble-wall trajectory in the phase plane (R_*, R'_*) is represented by the dash-and-dot line (in fact a single line, which appears interrupted in the figure because the minimum is out of scale). The lines representing the velocity fields in the liquid at every instant of time should issue from this dash-and-dot line from the particular point (R_*, R'_*) corresponding to that instant. For the instant to which the figure refers this value is at the common origin of the two continuous curves marked (a) and (b) (to be discussed at the end of this section). Clearly, the dashed line comes nowhere close to the correct boundary value for the velocity.

The source of the problem, and a possible remedy, are clearly seen by differentiating, (9.1a) to obtain the velocity at R_*:

$$u_*^{(0)}(R_*, t_*) = R'_* + \frac{1}{R_*}[G'_0(t_*+\epsilon R_*)+G'_0(t_*-\epsilon R_*)] - \frac{1}{\epsilon R_*^2}[G_0(t_*+\epsilon R_*)-G_0(t_*-\epsilon R_*)]. \tag{9.2}$$

Although the terms containing G_0 cancel in the limit $\epsilon \to 0$, an error remains for finite ϵ. This error would not arise if the argument of G_0 were

$$\tau_\pm = t_* \pm \epsilon[r_* - R_*(t_*)], \tag{9.3}$$

rather than $t_* \pm \epsilon r_*$. This dependence can be obtained by setting $t_* \pm \epsilon r_* = \tau_\pm \pm \epsilon R_*$ in (9.1) and expanding in Taylor's series centred about $\tau_\pm$. The result is

$$\varphi_*^{(0)} = \frac{1}{\epsilon r_*}[G_0(\tau_+)-G_0(\tau_-)]-\frac{1}{r_*}\{f_0(t_*)-R_*(t_*)[G'_0(\tau_+)+G'_0(\tau_-)]\}+\alpha_0, \tag{9.4a}$$

$$h_*^{(0)} = -\frac{1}{\epsilon r_*}[G'_0(\tau_+)-G'_0(\tau_-)]-\frac{R_*}{r_*}[G''_0(\tau_+)+G''_0(\tau_-)]+\frac{f'_0(t_*)}{r_*}-\frac{1}{2}\frac{f_0^2(t_*)}{r_*^4}. \tag{9.4b}$$

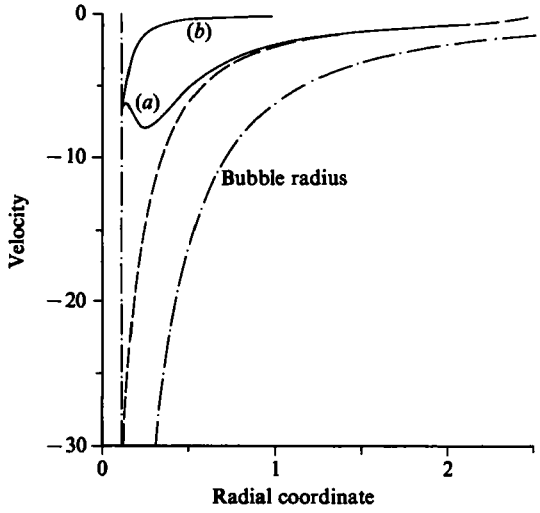

FIGURE 1. Dimensionless liquid velocity in the neighbourhood of the bubble according to the first-order composite expansion (9.5*a*) (curve *a*) and to the first-order inner result (6.15*a*) (curve *b*) during the deceleration phase near the end of the first collapse. The dashed line is the result of a first-order composite expansion similar to (9.1*a*). The dash-and-dot line is the bubble wall trajectory in the (R_*, R'_*) plane, the minimum of which is out of scale. These results are for a bubble in free collapse with initial conditions $R_*(0) = 4$, $R'_*(0) = 0$ at time $t_* = 3.6824$ at which $R_* = 0.117$, $R'_* = -6.89$.

In a similar manner the following expansions valid to $O(\epsilon)$ are found:

$$\varphi_*^{(1)} = \frac{1}{\epsilon r_*}[G_0(\tau_+) - G_0(\tau_-)] + \frac{R_*}{r_*}[G'_0(\tau_+) + G'_0(\tau_-)] - \frac{f_0(\tau_-)}{r_*} + \epsilon\frac{R_*}{r_*}\{\tfrac{1}{2}R_*[G''_0(\tau_+) - G''_0(\tau_-)] + f'_0(\tau_-)\} + \alpha_0, \quad (9.5a)$$

$$h_*^{(1)} = -\frac{1}{\epsilon r_*}[G'_0(\tau_+) - G'_0(\tau_-)] - \frac{R_*}{r_*}[G''_0(\tau_+) + G''_0(\tau_-)] + \frac{f'_0(\tau_-)}{r_*} - \frac{1}{2}\frac{f_0^2(t_*)}{r_*^4} - \epsilon\frac{R_*}{r_*}\{\tfrac{1}{2}R_*[G'''_0(\tau_+) - G'''_0(\tau_-)] + f''_0(\tau_-)\}, \quad (9.5b)$$

where $f_0 = R_*^2 R'_*$ and all the R_* have argument t_*. The corresponding results at $O(\epsilon^2)$ are very complicated and for simplicity we give the corresponding expressions only for the free case in which $G_0 = 0$. One has

$$\varphi_*^{(2)} = -\frac{f_0(\tau_-)}{r_*} + \epsilon\frac{R_*}{r_*}f_0(\tau_-) - \epsilon^2\left[\frac{1}{2}\frac{R_*^2}{r_*}f''(\tau_-) + \frac{f_2(t_*)}{r_*} - \frac{f_0(t_*)f'_0(t_*)}{r_*^2} + \frac{f_0^3(t_*)}{10r_*^5}\right], \quad (9.6a)$$

$$h_*^{(2)} = \frac{f'_0(\tau_-)}{r_*} - \frac{1}{2}\frac{f_0^2(t_*)}{r_*^4} - \epsilon\frac{R_*}{r_*}f''_0(\tau_-) + \epsilon^2\left\{\frac{1}{2}\frac{R_*^2}{r_*}f'''_0(\tau_-) + \frac{f'_2(t_*)}{r_*} - [\tfrac{1}{2}f_0(t_*)f'''_0(t_*) + f_0'^2(t_*)]\frac{1}{r_*^2} - \frac{f_0(t_*)f_2(t_*)}{r_*^4} + \frac{23}{10}\frac{f_0^2(t_*)f'_0(t_*)}{r_*^5} - \frac{f_0^4(t_*)}{2r_*^8}\right\}. \quad (9.6b)$$

where f_2 is given by (7.20).

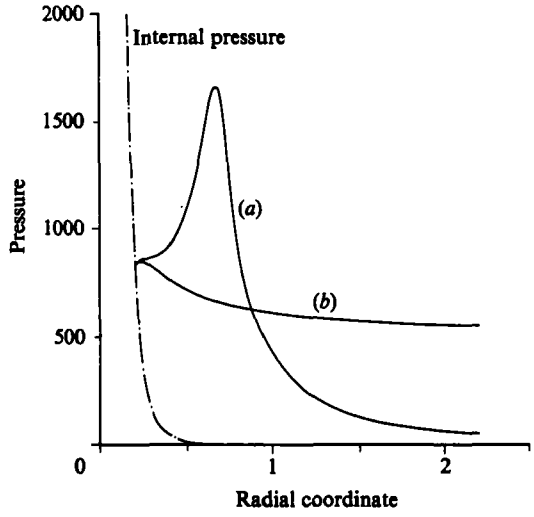

FIGURE 2. Normalized pressure field in the neighbourhood of the bubble for the same conditions as in the previous figure. Curve (*a*) is the composite expansion and curve (*b*) the inner result. The dash-and-dot line is the liquid pressure just outside the bubble plotted as a function of R_*. The pressure is referred to the undisturbed pressure at infinity.

The actual evaluation of the above expressions runs into the same difficulties encountered in the derivation of the radial equations due to the appearance of derivatives of the function $f_0 = R_*^2 R'_*$. These quantities can be evaluated in a variety of ways all equivalent to a certain order in ϵ. However some care is necessary to avoid inconsistencies between the limit form of the expressions as $r_* \to R_*$ and the values at the boundary. For the first-order enthalpy field (9.5*b*) we evaluate $\epsilon f_0'''$ from the first-order equation in the form (6.19) to find

$$h_*^{(1)} = -\frac{G_0'(\tau_+) - G_0'(\tau_-)}{\epsilon r_*} + h_{B*}(\tau_-)\frac{R_*(t_*)}{r_*}$$
$$+\frac{R_*}{r_*}[G_0''(\tau_-) - G_0''(\tau_+)] + \left[1 - \frac{R_*(t_*)}{R_*(\tau_-)}\right]\frac{f_0'(\tau_-)}{r_*}$$
$$-\frac{1}{2}\left[\frac{f_0^2(t_*)}{r_*^4} - \frac{f_0^2(\tau_-)}{R_*^4(\tau_-)}\frac{R_*(t_*)}{r_*}\right] - \epsilon\frac{R_*^2(t_*)}{2r_*}[G_0'''(\tau_+) - G_0'''(\tau_-)]. \qquad (9.5c)$$

It is readily verified that for $r_* = R_*$, $h_*^{(1)}$ equals h_{B*}. A similar procedure can be developed for the second-order fields (9.6) but the formulae are very involved and will not be given.

The practical implications of using the composite expansion for the fields can be appreciated in the example of figure 1 where the solid line marked (*a*) is obtained from the composite expansion (9.5*a*) while the one marked (*b*) is the inner field (6.15*a*). As already noted the dash-and-dot line is the bubble-wall trajectory in the phase plane (R_*, R'_*). The velocity fields are shown during the deceleration phase immediately before the end of the first collapse (for the exact conditions of the calculation see the caption to fig. 1). The composite expansion (line *a*) clearly shows the presence of the compression wave caused by the deceleration of the motion, which is absent from the inner, essentially incompressible, result (line *b*). The same features can be observed in figure 2 where the pressure distribution is shown.

10. Numerical results

Some general features of the dynamics of a freely oscillating bubble are illustrated in figures 3 and 4 where the radius and the radial velocity are shown as a function of time. Here, as in all the subsequent results, the internal pressure is given by the adiabatic expression

$$p_i = p_{i0}\left(\frac{R_0}{R}\right)^{3\gamma}, \tag{10.1}$$

where γ is the ratio of the specific heats of the gas, R_0 is the equilibrium radius, also used as the unit of length, and p_{i0} is the equilibrium internal pressure given by

$$p_{i0} = p_\infty + \frac{2\sigma}{R_0}, \tag{10.2}$$

The velocity unit introduced in (3.1) is

$$U = \left(\frac{p_\infty}{\rho_\infty}\right)^{\frac{1}{2}}. \tag{10.3}$$

In all the examples we take the following numerical values: $\gamma = 1.4$, $p_\infty = 1$ bar, $\rho_\infty = 0.998$ g/cm, $\mu = 0.01\,P$, $\sigma = 72.5\,\mathrm{erg/cm^2}$, $R_0 = 0.01$ cm, $B = 3049$ bar, $n = 7.15$. With these we find $c_\infty = 1478.2$ m/s, $U = 10.010$ m/s, $T = 10$ μs, $c_{\infty *} = 147.67$. It can readily be verified that, after the non-dimensionalizations (3.1) and (8.11), dimensional quantities enter only through the parameter ϵ and

$$M_1 = \frac{2\sigma}{R_0 p_\infty}, \quad M_2 = \frac{4\mu U}{R_0 p_\infty}, \tag{10.4}$$

which, with the previous values, are $M_1 = 0.0145$ and $M_2 = 4.00 \times 10^{-5}$. Since both parameters are important only when they are of order one, it may be concluded that the results to be shown are typical of sufficiently large bubbles for which the effect of M_1 and M_2 is negligible.

The initial conditions for figures 1–8 are $R_*(0) = 4$, $R'_*(0) = 0$. In figure 3 the result of the Rayleigh–Plesset equation (5.17) (dash and dot line) is compared with the first-order equation (6.18) (dashed line) and the second-order equation (8.9) with $\lambda = 0.5$, $\theta = 0$ (solid line). The energy lost by radiation is seen to be quite large and the Rayleigh–Plesset equation, although very accurate during the first collapse, grossly overpredicts the rebound and the period of oscillation. The difference between the first- and second-order results is much smaller, with the first-order equation slightly overpredicting the amount of energy radiated. This leads to smaller maximum radii and consequently somewhat shorter periods of oscillation. This is confirmed by figure 4 which shows the radial velocity in the vicinity of the second minimum of figure 3 as predicted by the same first- and second-order equations.

Figures 5–11 are devoted to a comparison of the approximate results obtained in this paper with those given by a direct numerical integration of the exact partial differential formulation. These 'exact' numerical results are the same as those presented in I and no details about the numerical method will be repeated here. We only recall that, for reasons of economy, the numerical integration was started at a time $\bar{t}_* > 0$ using the composite expansions (9.5) to determine the initial distribution of the potential and enthalpy fields in the liquid.

The error of the approximations made is most evident at high velocity or high pressure, both of which are found in the neighbourhood of the radius minima [cf.

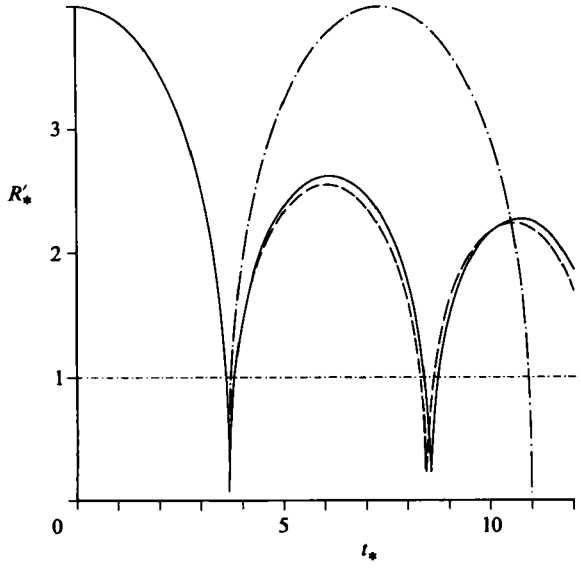

FIGURE 3. Bubble radius as a function of time for free oscillations with initial conditions $R_*(0) = 4$, $R'_*(0) = 0$. The solid line is the result given by the second-order equation (8.9) with $\lambda = 0.5$, $\theta = 0$. The dashed line is according to the first-order equation (6.18), and the dash-and-dot line is the zero-order Rayleigh–Plesset equation (5.17).

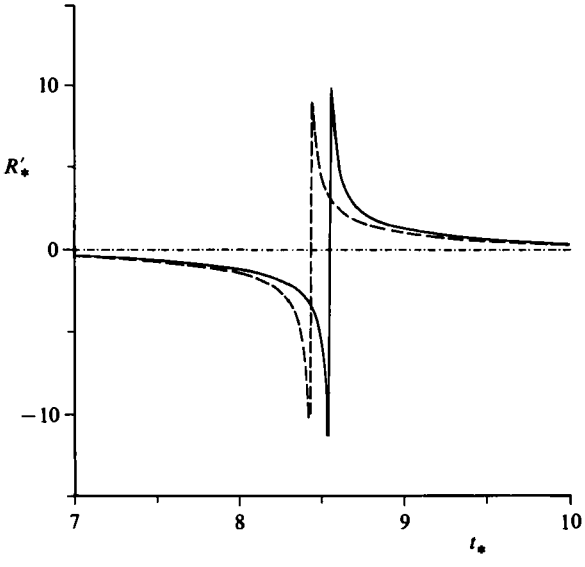

FIGURE 4. Dimensionless radial velocity as a function of time in the vicinity of the second minimum of the previous figure. The solid and the dashed lines are according to the second- and first-order equations, respectively.

figure 4 and (10.1)]. As in I we consider the values predicted by the different second-order equations for the first minimum radius, the minimum velocity during the first collapse (which is a maximum in absolute value), and the maximum velocity during the first rebound. Shortly after this point of maximum velocity a shock wave is formed in the liquid and the numerical method used, based on the characteristics of

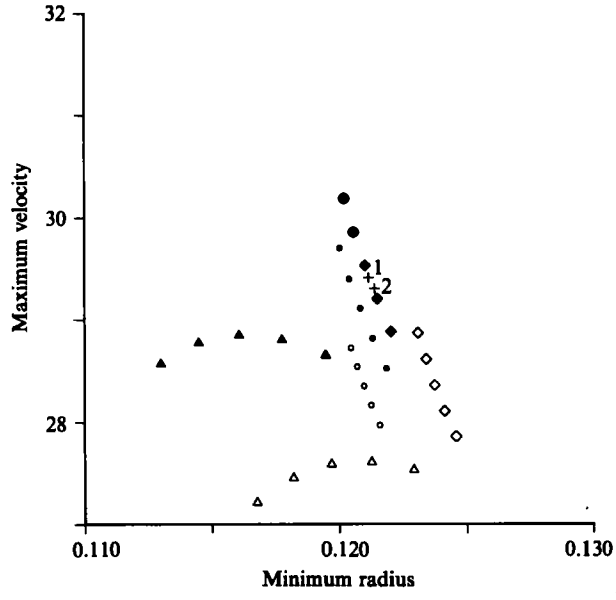

FIGURE 5. Dimensionless maximum velocity attained during the first rebound versus the dimensionless minimum radius at the end of the preceding collapse (which is completed at a dimensionless time close to 3.68 depending on the equation used) for the initial conditions $R_*(0) = 4$, $R'_*(0) = 0$. The crosses are the 'exact' numerical results obtained starting from $t_* = 3.6653$, $R_* = 0.5522$, $R'_* = -14.26$ (point 1) and starting from $t_* = 3.6250$, $R_* = 0.9322$, $R'_* = -6.863$ (point 2). The other points are the results obtained from the approximate ordinary differential equations. The filled symbols are for equations written in terms of the enthalpy, the open ones in terms of the pressure. Triangles: first-order equations with, from right to left, $\lambda = 1, 0.75, 0.5, 0.25, 0$. Diamonds: second-order equations quadratic in the radial acceleration. Circles: second-order equations after the substitution (8.8*a*). For the second-order equations $\theta = 0$ and λ as above, decreasing downwards.

the system, ceases to be applicable. In all the figures black symbols refer to results obtained from equations written in terms of the enthalpy and open symbols to results obtained from equations written in terms of the pressure.

Figure 5 shows the maximum dimensionless velocity plotted as a function of the minimum radius. The 'exact' numerical results are indicated by the two crosses which correspond to different starting conditions. We include two such results to give an indication of the error that can be expected to affect the numerical calculation. The triangles are results predicted by the first-order equations (6.19) in terms of the enthalpy (black triangles) and of the pressure (i.e. the same equation with p_{B*} in place of h_{B*}, cf. (8.10), open triangles), and are identical with those of figure 1 of I. The circles are obtained from the second-order equation (8.9) written in terms of the enthalpy (solid symbols) or in terms of the pressure (open symbols). The diamonds are obtained from the second-order form (8.7) treated as a quadratic in R''_* and solved analytically for this quantity. The first-order results have been obtained with (from left to right) $\lambda = 1$, 0.75, 0.5, 0.25, 0 and the second-order ones with $\theta = 0$ and the same values of λ (increasing upwards).

A first qualitative comment is that all the second-order results tend to be closer to the 'exact' ones than the first-order results and tend to exhibit a somewhat smaller scatter. For the reasons mentioned in §3 and in I use of the enthalpy also proves beneficial, and decreases the difference between the forms linear and quadratic in

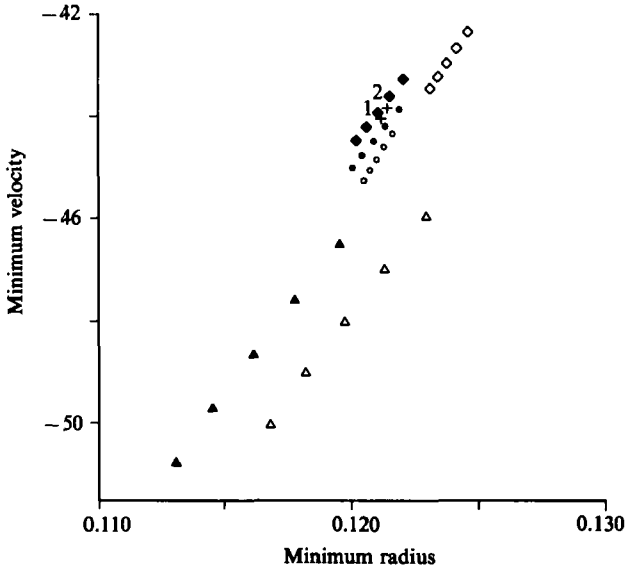

FIGURE 6. Dimensionless minimum velocity (maximum in absolute value) during the first collapse versus the dimensionless minimum radius at the end of the collapse for the same cases as in the previous figure. Again $\theta = 0$ and $\lambda = 1$, 0.75, 0.5, 0.25, 0 decreasing upward for each family of points. The crosses are the 'exact' numerical results.

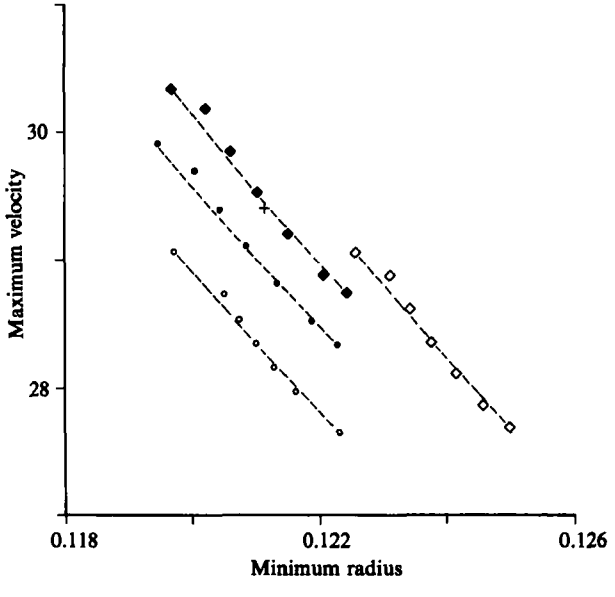

FIGURE 7. Effect of varying the parameter θ on the results of figure 5. The three points connected by the dashed lines correspond to $\lambda = 0.5$, $\theta = 1$ (upper left), $\lambda = 0.5$, $\theta = 0$ (middle), and $\lambda = 0.5$, $\theta = -1$ (lower right). Results for intermediate values of θ fall along the dashed lines. The other points are those for $\theta = 0$ already shown in figure 5. The cross is the 'exact' numerical result (point 1 in figure 5).

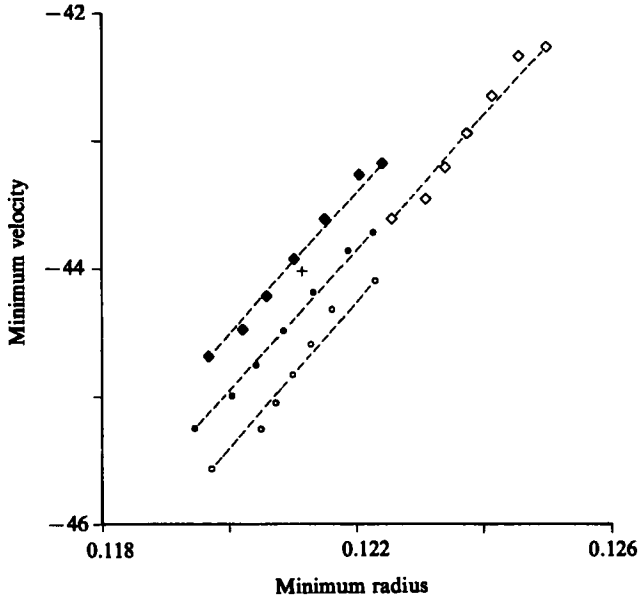

FIGURE 8. Effect of varying the parameter θ on the results of figure 6. The parameter θ goes from 1 to -1 describing the dashed lines from left to right. See the caption to the preceding figure.

R''_*. The same conclusions can be drawn from figure 6, in which the minimum dimensionless velocity during the first collapse (maximum in absolute value) is plotted versus the minimum radius. It is clear from figure 6 that the excessive radiated energy predicted by the first-order equations is a consequence of a more violent collapse which leads to a higher maximum pressure. In figures 7 and 8 we demonstrate the effect of varying the second parameter θ on the results of figures 5 and 6. In both figures the dashed lines go through the points corresponding to ($\lambda = 0.5$, $\theta = 1$, left), ($\lambda = 0.5$, $\theta = 0$), and ($\lambda = 0.5$, $\theta = -1$, right) and indicate the trend of the results for $-1 \leqslant \theta \leqslant 1$. The other points are for $\theta = 0$ and, from left to right, $\lambda = 1, 0.75, 0.5, 0.25$ and 0, as before. The first-order points have been omitted. These and other similar results indicate that a value of θ close to zero is optimal, at least for the cases investigated.

Figures 9 and 10 are similar to figures 5 and 6 but for an initial value of the radius $R_*(0) = 6$. Such a large value is probably unrealistic because the bubble would most likely shatter before rebounding, but these results are useful to confirm the trends found in the previous case since here the maximum Mach number is close to 1. Finally, figure 11 is for $R_*(0) = 3$. Here, the maximum Mach number is approximately 0.13 and all the second-order results lie very close to each other.

Some results for a case of forced motion are shown in figure 12. The incident wave has the same form used in I, namely

$$G_0(t_*) = \tfrac{1}{4}(2\pi)^{\frac{1}{2}} A\tau(t_* - t_0)\,\mathrm{erf}\left(\frac{t_* - t_0}{\tau\sqrt{2}}\right) + \tfrac{1}{2}A\tau^2 \exp\left[-\frac{(t_* - t_0)^2}{2\tau^2}\right], \qquad (10.5)$$

with $A = -300$, $\tau = 0.01$, and $t_0 = 0.447\,66$. A graph of the radius as a function of time for this case is shown in figure 13. The dash-and-dot line is the zero-order result (5.17), the dashed line is the first-order result (6.18), and the continuous line is the

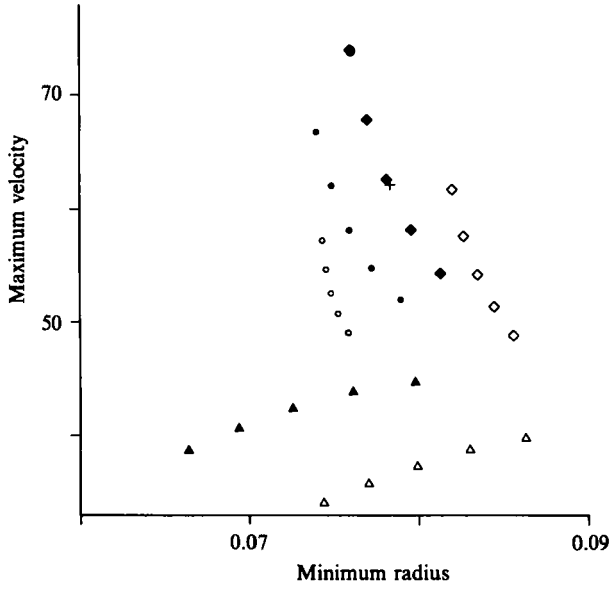

FIGURE 9. Same as figure 5 for $R_*(0) = 6$. The parameter λ has the values 1, 0.75, 0.5, 0.25, 0 from left to right for the triangles (first-order equations) and from top down for the second-order points. $\theta = 0$ for the latter. See caption to figure 5.

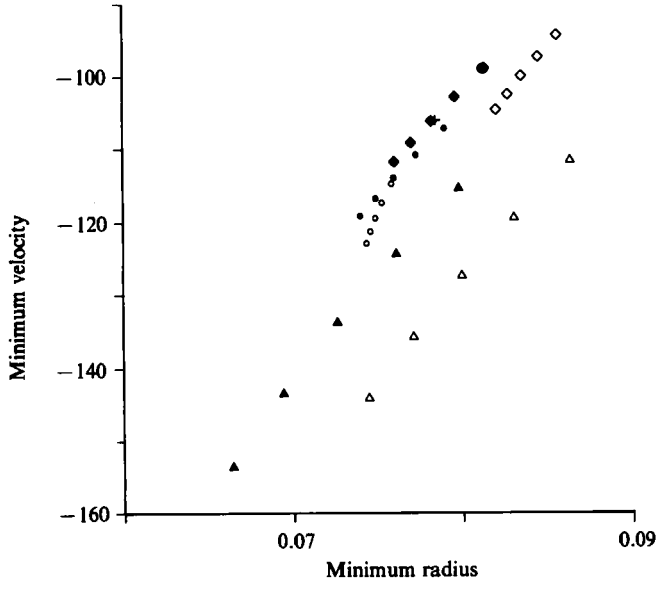

FIGURE 10. Same as figure 6 for $R_*(0) = 6$. The parameter λ has the values 1, 0.75, 0.5, 0.25, 0 from left to right, for all families of points, and $\theta = 0$. The 'exact' numerical result has been obtained starting the numerical integration from $R_* = 0.831$, $R'_* = -14.668$.

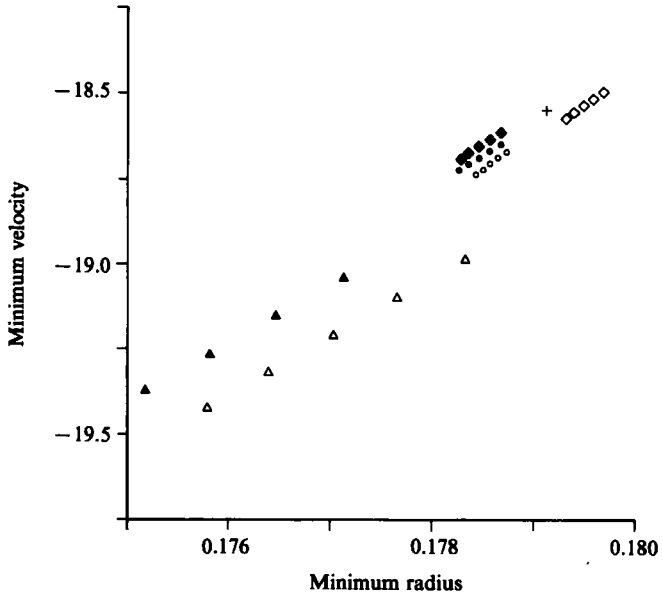

FIGURE 11. Same as figures 6 and 10 but for $R_*(0) = 3$. The filled triangle corresponding to $\lambda = 1$ is out of scale and is not included. The cross is the 'exact' numerical result obtained starting from $R_* = 0.8458$, $R' = -5.016$.

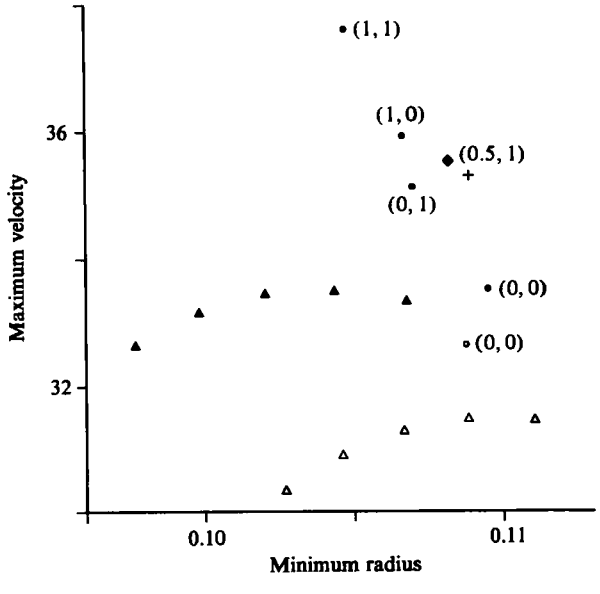

FIGURE 12. Same as figures 5 and 9, but for the forced-collapse case. The first-order results (triangles) are for $\lambda = 1, 0.75, 0.5, 0.25, 0$ from left to right. The parameter values for the second-order results are indicated in parentheses as (λ, θ). The cross is the 'exact' numerical result.

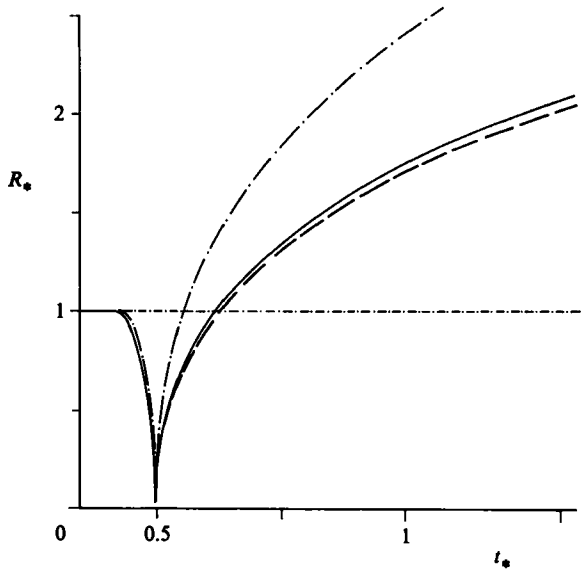

FIGURE 13. Normalized bubble radius as a function of time for the forced-collapse case. The solid line is the second-order equation (8.7) with $\lambda = 0.5$, $\theta = 0$, the dashed line is the first-order equation (6.18), and the dash-and-dot line is the zero-order equation (5.17).

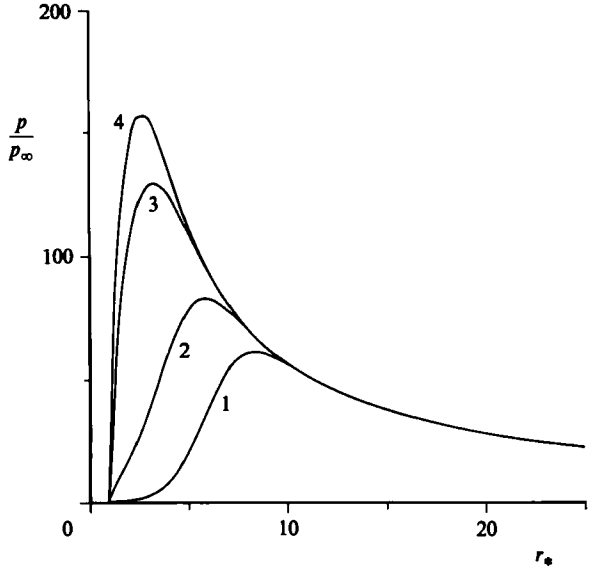

FIGURE 14. Pressure distribution in the liquid in the forced-motion case computed numerically from the partial differential formulation at times 0.40452 (curve 1), 0.41874 (curve 2), 0.43218 (curve 3), 0.44233 (curve 4). The corresponding values of the bubble wall velocity are -0.001, -0.1, -1.47, -4.41.

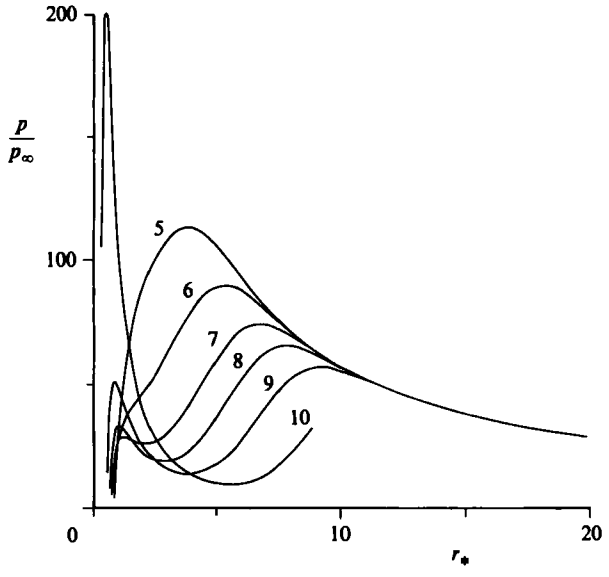

FIGURE 15. Same as in the previous figure for $t_* = 0.45246$, $R'_* = -7.35$ (curve 5), $t_* = 0.45957$, $R'_* = -8.82$ (curve 6), $t_* = 0.46734$, $R'_* = -10.3$ (curve 7), $t_* = 0.47353$, $R'_* = -11.76$ (curve 8), $t_* = 0.48154$, $R'_* = -14.7$ (curve 9), and $t_* = 0.49404$, $R'_* = -29.4$ (curve 10).

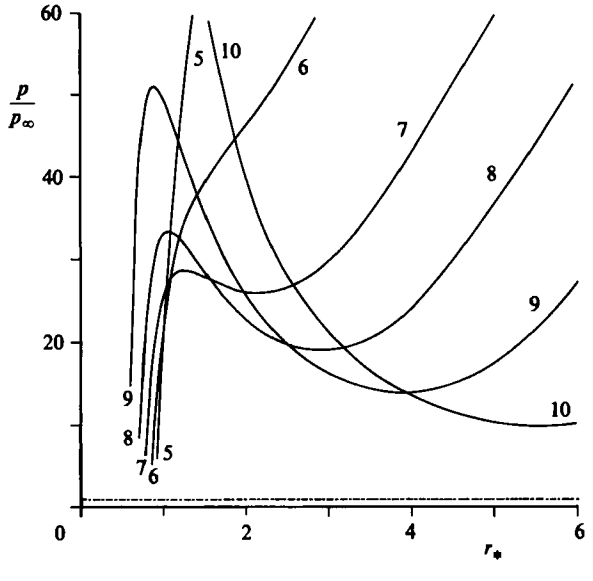

FIGURE 16. Enlargement of the lower left-hand corner of figure 15. For the key to the numbering of the curves see the caption to figure 15. The dashed line is the undisturbed value of the pressure.

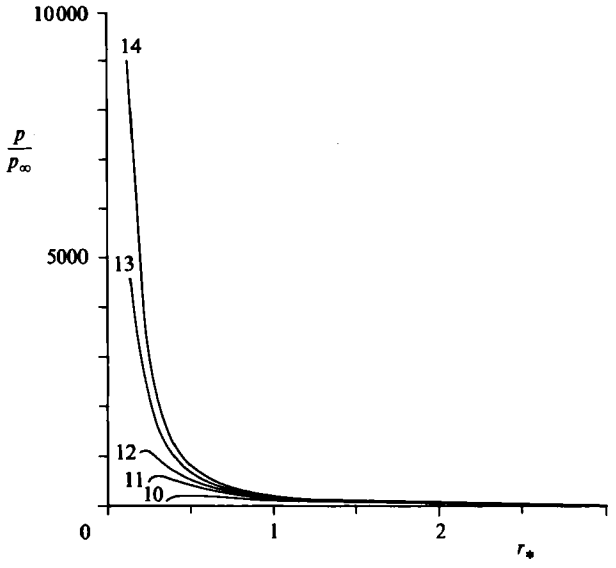

FIGURE 17. Continuation of figures 14 and 15. Note the change in both scales. The curves are for $t_* = 0.49404$, $R'_* = -29.4$ (curve 10; this curve is also shown in figures 15 and 16), $t_* = 0.49716$, $R'_* = -44.4$ (curve 11), $t_* = 0.49807$, $R'_* = -51.4$ (curve 12), $t_* = 0.49916$, $R'_* = -51.4$ (curve 13; the minimum velocity is attained between these two instants), $t_* = 0.49965$, $R'_* = -29.4$ (curve 14).

second-order result (8.7) with $\lambda = 0.5$, $\theta = 0$. The comparison among the different approximations is similar to that in figure 3.

We conclude this section with an illustration of the pressure field in the liquid in the forced case as calculated numerically; similar results for free collapse are already available in the literature (Hickling & Plesset 1964; Fujikawa & Akamatsu 1980). Figure 14 shows the incident pressure pulse (10.5) at different instants as it moves towards the bubble and grows owing to geometrical focusing. The maximum is reached near $t_* = 0.44233$ (curve 4), after which the pulse is reflected (figure 15). It is only at this time that significant motion and pressure disturbances begin to develop near the bubble as is particularly clear in figure 16 which is an enlargement of the lower left-hand corner of figure 15. Once set into inward motion, the bubble continues to compress seemingly independently of the external pressure field. The internal pressure gradually builds up reaching a maximum value more than 9000 times the initial one (figure 17; note the change in the vertical scale).

It has not been possible to compare the numerical results with the composite expansions for the fields given in the previous section in a meaningful way because the motion is too rapid. For example, in figure 17 the top two lines correspond to $t_* = 0.499165$ and 0.499650 respectively. At a fixed time, therefore, even a slight difference in phase between the analytical and numerical solutions (caused, for instance, by slightly different starting conditions for the latter, cf. caption to figure 5) can give rise to large discrepancies of little significance. On the other hand, since the fields depend on the history of the motion, it is difficult to justify criteria for comparison other than at equal time.

11. Conclusions

On the basis of the limited number of cases for which the 'exact' numerical solution has been compared with the approximate one we can now attempt to draw some tentative conclusions. The first point concerns whether use of one of the second-order equations which, especially in the forced case, are much more complex than the first-order ones, is warranted by the associated gain in accuracy. The answer is probably negative unless the maximum Mach number reached by the bubble wall exceeds 0.5 or the internal pressure exceeds 5000 times the undisturbed value. It was found in I that the value $\lambda = 0$, corresponding to the Keller form, resulted in a close-to-optimal first-order equation. The dimensional form of this equation is

$$\left(1-c_\infty^{-1}\frac{\mathrm{d}R}{\mathrm{d}t}\right)R\frac{\mathrm{d}^2R}{\mathrm{d}t^2}+\frac{3}{2}\left(1-\tfrac{1}{3}c_\infty^{-1}\frac{\mathrm{d}R}{\mathrm{d}t}\right)\left(\frac{\mathrm{d}R}{\mathrm{d}t}\right)^2 = \left(1+c_\infty^{-1}\frac{\mathrm{d}R}{\mathrm{d}t}+c_\infty^{-1}R\frac{\mathrm{d}}{\mathrm{d}t}\right)\left(h_B-\frac{p(t)-p_\infty}{\rho_\infty}\right),$$

where h_B is given by (2.10) and $p(t)$ is the (spherically symmetric part of the) liquid pressure at the bubble site in the absence of the bubble. If, however, a second-order equation is to be used, our results seem to indicate that parameter values close to ($\lambda = 0.5$, $\theta = 0$) and the form (8.7) quadratic in the acceleration give good results. The dimensional form of this equation is

$$\begin{aligned}&\left(c_\infty^{-1}R\frac{\mathrm{d}^2R}{\mathrm{d}t^2}\right)^2+\left[1-\tfrac{3}{2}c_\infty^{-1}\frac{\mathrm{d}R}{\mathrm{d}t}\left(1-\tfrac{38}{15}c_\infty^{-1}\frac{\mathrm{d}R}{\mathrm{d}t}\right)\right]R\frac{\mathrm{d}^2R}{\mathrm{d}t^2}\\&\quad+\frac{3}{2}\left[1-\tfrac{5}{6}c_\infty^{-1}\frac{\mathrm{d}R}{\mathrm{d}t}\left(1-\tfrac{52}{25}c_\infty^{-1}\frac{\mathrm{d}R}{\mathrm{d}t}\right)\right]\left(\frac{\mathrm{d}R}{\mathrm{d}t}\right)^2\\&=\left(1+\tfrac{1}{2}c_\infty^{-1}\frac{\mathrm{d}R}{\mathrm{d}t}\right)\left[h_B-\frac{p(t)-p_\infty}{\rho_\infty}\right]\\&\quad+c_\infty^{-1}\left(1-\tfrac{3}{2}c_\infty^{-1}\frac{\mathrm{d}R}{\mathrm{d}t}\right)R\frac{\mathrm{d}}{\mathrm{d}t}\left[h_B-\frac{p(t)-p_\infty}{\rho_\infty}\right]\\&\quad+c_\infty^{-2}\frac{\mathrm{d}}{\mathrm{d}t}\left[g_2-R^2\frac{\mathrm{d}}{\mathrm{d}t}\frac{p(t)-p_\infty}{\rho_\infty}\right],\end{aligned}$$

where g_2 is given by (7.22). In any case, equations containing the enthalpy should be preferred.

It should be stressed that these conclusions have been arrived at on the basis of a limited number of examples. Although these appear to be representative of situations of practical interest it should be borne in mind that the effect of shock-wave formation in the liquid has not been examined. Hence, for example, it is impossible to assess the accumulated error affecting the approximate equations after a number of repeated oscillations.

The only second-order equations available before this work were the ones derived by Tomita & Shima (1977) and the related one by Fujikawa & Akamatsu (1980). These equations are in terms of the pressure, rather than the enthalpy, and are not quadratic in the bubble-wall acceleration. Furthermore, they are applicable only to the case of free motion. Other equations containing some, but not all, second-order

terms have been proposed. Those of Flynn (1975) and Rath (1980) are, in this respect, very incomplete. When second-order terms are dropped they reduce to the Keller and Herring forms, respectively, written in terms of the pressure. Tilmann (1980) has derived an equation in terms of the enthalpy similar to our (8.7) with $\lambda = 0, \theta = 2$. The only differences are that the substitution (8.8*b*) is used and that the terms $\epsilon^2[G_0^{\mathrm{iv}} R_*^2 + g_2']$ do not appear. Except for this second feature, which has an effect only in the case of forced motion, Tilmann's equation is therefore a valid second-order approximate equation. Another equation containing the enthalpy was given by Gilmore (1952). This equation has already been discussed in I where it was shown to be a poorer approximation than the first-order Keller equation. From a consideration of our results it appears that the strongest reason for its apparent success noted by Hickling & Plesset (1964) is the use of the enthalpy rather than the pressure.

The present study has been supported in part by the Courant Institute of Mathematics, New York University, through the grant ONR N00014-81-K-0002.

Appendix A

Here we give details of the solution procedure at first order carried out in §6. The exact equations found upon substitution of (6.1) into (3.7), (3.8) are

$$\begin{aligned}\nabla_*^2\varphi_1 = \epsilon&\left[\frac{\partial^2\varphi_0}{\partial t_*^2} + 2\frac{\partial\varphi_0}{\partial r_*}\frac{\partial^2\varphi_0}{\partial r_*\,\partial t_*} + \left(\frac{\partial\varphi_0}{\partial r_*}\right)^2\frac{\partial^2\varphi_0}{\partial r_*^2}\right]\\ &+\epsilon^2\left\{\frac{\partial^2\varphi_1}{\partial t_*^2} + 2\left(\frac{\partial\varphi_0}{\partial r_*}\frac{\partial^2\varphi_1}{\partial r_*\,\partial t_*} + \frac{\partial\varphi_1}{\partial r_*}\frac{\partial^2\varphi_0}{\partial r_*\,\partial t_*} + \frac{\partial\varphi_0}{\partial r_*}\frac{\partial\varphi_1}{\partial r_*}\frac{\partial^2\varphi_0}{\partial r_*^2}\right)\right.\\ &\left.+\left(\frac{\partial\varphi_0}{\partial r_*}\right)^2\frac{\partial^2\varphi_1}{\partial r_*^2} + (n-1)\left[\frac{\partial\varphi_0}{\partial t_*} + \frac{1}{2}\left(\frac{\partial\varphi_0}{\partial r_*}\right)^2\right]\nabla_*^2\varphi_1\right\}\\ &+\epsilon^3\left[2\frac{\partial\varphi_1}{\partial r_*}\frac{\partial^2\varphi_1}{\partial r_*\,\partial t_*} + 2\frac{\partial\varphi_0}{\partial r_*}\frac{\partial\varphi_1}{\partial r_*}\frac{\partial^2\varphi_1}{\partial r_*^2} + \left(\frac{\partial\varphi_1}{\partial r_*}\right)^2\frac{\partial^2\varphi_0}{\partial r_*^2}\right.\\ &\left.+(n-1)\left(\frac{\partial\varphi_1}{\partial t_*} + \frac{\partial\varphi_0}{\partial r_*}\frac{\partial\varphi_1}{\partial r_*}\right)\nabla_*^2\varphi_1\right]\\ &+\epsilon^4\left[\left(\frac{\partial\varphi_1}{\partial r_*}\right)^2\frac{\partial^2\varphi_1}{\partial r_*^2} + \tfrac{1}{2}(n-1)\left(\frac{\partial\varphi_1}{\partial r_*}\right)^2\nabla_*^2\varphi_1\right],\end{aligned} \tag{A 1a}$$

$$\frac{\partial\varphi_1}{\partial t_*} + \frac{\partial\varphi_0}{\partial r_*}\frac{\partial\varphi_1}{\partial r_*} + h_1 + \tfrac{1}{2}\epsilon\left(\frac{\partial\varphi_1}{\partial r_*}\right)^2 = 0. \tag{A 1b}$$

Upon introduction of the scaled variable (4.2) $r_\eta = \eta(\epsilon) r_*$, with η constrained to belong to the zero-order inner domain (5.7), these equations take a form which can schematically be indicated as follows:

$$\nabla_\eta^2\varphi_1 = \frac{\epsilon}{\eta^2}\left[2G_0''' + O(\eta)\right] + \frac{\epsilon^2}{\eta^2}\frac{\partial^2\varphi_1}{\partial t_*^2} + O(\epsilon^2, \epsilon^4\eta^2), \tag{A 2a}$$

$$\frac{\partial\varphi_1}{\partial t_*} + h_1 + \eta^3\frac{f_0(t_*)}{r_\eta^2}\frac{\partial\varphi_1}{\partial r_\eta} + \tfrac{1}{2}\epsilon\eta^2\left(\frac{\partial\varphi_1}{\partial r_\eta}\right)^2 = 0. \tag{A 2b}$$

The first term in the right-hand side of (A 2a) arises from the term $\epsilon\,\partial^2\varphi_0/\partial t_*^2$ in (A 1a), and only the leading orders of the remaining terms have been indicated.

The formal limits of the system (A 2) are

$$\nabla^2\varphi_1 = 0, \quad \frac{\partial\varphi_1}{\partial t_*}+\frac{f_0}{r_*^2}\frac{\partial\varphi_1}{\partial r_*}+h_1 = 0, \quad \text{ord}\,\eta = \text{ord}\,1, \tag{A 3}$$

$$\nabla_\eta^2\varphi_1 = 0, \quad \frac{\partial\varphi_1}{\partial t_*}+h_1 = 0, \quad \text{ord}\,\epsilon^{\frac{1}{3}} < \text{ord}\,\eta < \text{ord}\,1, \tag{A 4}$$

$$\nabla_\eta^2\varphi_1 = 2G_0''', \quad \frac{\partial\varphi_1}{\partial t_*}+h_1 = 0, \quad \text{ord}\,\eta = \text{ord}\,\epsilon^{\frac{1}{3}}, \tag{A 5}$$

$$O = 2G_0''', \quad \frac{\partial\varphi_1}{\partial t_*}+h_1 = 0, \quad \text{ord}\,\epsilon < \text{ord}\,\eta < \text{ord}\,\epsilon^{\frac{1}{3}}. \tag{A 6}$$

Clearly, (A 3) contains (A 4) and (A 5) contains both (A 4) and (A 6). Therefore (A 3) and (A 5) are the distinguished limits given in §6 as (6.2) and (6.3) and their domain of overlap is the domain of validity of (A 4) given in (6.5).

In a similar way the introduction of (6.7) into (3.7), (3.8) leads to

$$\begin{aligned}
\nabla_*^2\phi_1 = {}&\epsilon\left\{2\frac{\partial\phi_0}{\partial r_*}\frac{\partial^2\phi_0}{\partial r_*\,\partial t_*}+\left(\frac{\partial\phi_0}{\partial r_*}\right)^2\frac{\partial^2\phi_0}{\partial r_*^2}+(n-1)\left[\frac{\partial\phi_0}{\partial t_*}+\frac{1}{2}\left(\frac{\partial\phi_0}{\partial r_*}\right)^2\right]\nabla_*^2\phi_0\right\}\\
&+\epsilon^2\left\{\frac{\partial^2\phi_1}{\partial t_*^2}+2\left(\frac{\partial\phi_0}{\partial r_*}\frac{\partial^2\phi_1}{\partial r_*\,\partial t_*}+\frac{\partial\phi_1}{\partial r_*}\frac{\partial^2\phi_0}{\partial r_*\,\partial t_*}+\frac{\partial\phi_0}{\partial r_*}\frac{\partial\phi_1}{\partial r_*}\frac{\partial^2\phi_0}{\partial r_*^2}\right)\right.\\
&+\left(\frac{\partial\phi_0}{\partial r_*}\right)^2\frac{\partial^2\phi_1}{\partial r_*^2}+(n-1)\left[\frac{\partial\phi_0}{\partial t_*}+\frac{1}{2}\left(\frac{\partial\phi_0}{\partial r_*}\right)^2\right]\nabla_*^2\phi_1\\
&\left.+(n-1)\left[\frac{\partial\phi_1}{\partial t_*}+\frac{\partial\phi_0}{\partial r_*}\frac{\partial\phi_1}{\partial r_*}\right]\nabla_*^2\phi_0\right\}+\epsilon^3\left\{2\frac{\partial\phi_1}{\partial r_*}\frac{\partial^2\phi_1}{\partial r_*\,\partial t_*}+2\frac{\partial\phi_0}{\partial r_*}\frac{\partial\phi_1}{\partial r_*}\frac{\partial^2\phi_1}{\partial r_*^2}\right.\\
&+\left(\frac{\partial\phi_1}{\partial r_*}\right)^2\frac{\partial^2\phi_0}{\partial r_*^2}+(n-1)\left[\frac{\partial\phi_1}{\partial t_*}+\frac{\partial\phi_0}{\partial r_*}\frac{\partial\phi_1}{\partial r_*}\right]\nabla_*^2\phi_1\\
&\left.+\tfrac{1}{2}(n-1)\left(\frac{\partial\phi_1}{\partial r_*}\right)^2\nabla_*^2\phi_0\right\}\\
&+\epsilon^4\left[\left(\frac{\partial\phi_1}{\partial r_*}\right)^2\frac{\partial^2\phi_1}{\partial r_*^2}+\tfrac{1}{2}(n-1)\left(\frac{\partial\phi_1}{\partial r_*}\right)^2\nabla_*^2\phi_1\right],
\end{aligned} \tag{A 7a}$$

$$\epsilon H_1 = -\frac{1}{2}\left(\frac{\partial\phi_0}{\partial r_*}\right)^2-\epsilon\left(\frac{\partial\phi_1}{\partial t_*}+\frac{\partial\phi_0}{\partial r_*}\frac{\partial\phi_1}{\partial r_*}\right)-\tfrac{1}{2}\epsilon^2\left(\frac{\partial\phi_1}{\partial r_*}\right)^2. \tag{A 7b}$$

Again setting $r_\eta = \eta(\epsilon)\,r_*$, with η belonging now to the domain of validity (5.8) of the zero-order outer solution, one finds

$$\nabla_\eta^2\phi_1 = \frac{\epsilon^2}{\eta^2}\frac{\partial^2\phi_1}{\partial t_*^2}+O\left(\epsilon^2, \frac{\epsilon^3}{\eta^2}\right), \tag{A 8a}$$

$$\frac{\partial\phi_1}{\partial t_*}+H_1+O\left(\frac{\epsilon^3}{\eta^2}\right)+O\left(\epsilon^2, \epsilon\eta^2, \frac{\epsilon^3}{\eta^2}\right) = 0, \tag{A 8b}$$

for $\operatorname{ord}\epsilon \leqslant \operatorname{ord}\eta < \operatorname{ord}1$, while

$$\nabla_\eta^2 \phi_1 = \frac{\epsilon^2}{\eta^2}\frac{\partial^2 \phi_1}{\partial t_*^2} + O\left(\frac{\epsilon^2}{\eta}\right), \tag{A 9a}$$

$$\frac{\partial \phi_1}{\partial t_*} + H_1 + O\left(\frac{\eta^2}{\epsilon}\right) = 0, \tag{A 9b}$$

for $\operatorname{ord}\eta < \operatorname{ord}\epsilon$.

The formal limits of (A 8) are

$$\nabla_\eta^2 \phi_1 = 0, \quad \frac{\partial \phi_1}{\partial t_*} + H_1 = 0, \quad \operatorname{ord}\epsilon < \operatorname{ord}\eta < \operatorname{ord}1, \tag{A 10}$$

$$\tilde{\nabla}^2 \phi_1 = \frac{\partial^2 \phi_1}{\partial t_*^2}, \quad \frac{\partial \phi_1}{\partial t_*} + H_1 = 0, \quad \operatorname{ord}\epsilon = \operatorname{ord}\eta, \tag{A 11}$$

while from (A 9) we have

$$\frac{\partial^2 \phi_1}{\partial t_*^2} = 0, \quad \frac{\partial \phi_1}{\partial t_*} + H_1 = 0, \quad \operatorname{ord}\eta < \operatorname{ord}\epsilon. \tag{A 12}$$

The only distinguished limit is (A 11), since it contains both (A 10) and (A 12). This equation is therefore valid in the whole domain $\operatorname{ord}\eta < \operatorname{ord}1$.

Appendix B

Here we shall verify the correctness of the expression (7.15) as a particular solution of (7.7*a*). The second derivative of ψ with respect to $\tilde{r}$ may be written

$$\begin{aligned}\frac{\partial^2 \psi}{\partial \tilde{r}^2} &= \frac{1}{2}\int_0^{t_*} \mathrm{d}\tau \int_\tau^{t_*} \mathrm{d}\theta \left[\frac{\partial^2 \Gamma}{\partial \alpha^2}(\alpha,\tau)\bigg|_{\alpha=\tilde{r}-\theta+\tau} + \frac{\partial^2 \Gamma(\beta,\tau)}{\partial \beta^2}\bigg|_{\beta=\tilde{r}+\theta-\tau}\right] \\ &= \frac{1}{2}\int_0^{t_*} \mathrm{d}\tau \left[-\int_{\tilde{r}}^{\tilde{r}-t_*+\tau} \frac{\partial^2 \Gamma}{\partial \alpha^2}\mathrm{d}\alpha + \int_{\tilde{r}}^{\tilde{r}+t_*-\tau} \frac{\partial^2 \Gamma}{\partial \beta^2}\mathrm{d}\beta\right] \\ &= \frac{1}{2}\int_0^{t_*} \mathrm{d}\tau \int_{\tilde{r}-t_*+\tau}^{\tilde{r}+t_*-\tau} \frac{\partial^2 \Gamma}{\partial \alpha^2} d\alpha = \frac{1}{2}\int_0^{t_*} \frac{\partial \Gamma(\alpha,\tau)}{\partial \alpha}\bigg|_{\tilde{r}-t_*+\tau}^{\tilde{r}+t_*-\tau} \mathrm{d}\tau.\end{aligned} \tag{B 1}$$

Differentiating ψ with respect to time we find

$$\frac{\partial \psi}{\partial t_*} = \frac{1}{2}\int_0^{t_*} [\Gamma(\tilde{r}+t_*-\tau,\tau) + \Gamma(\tilde{r}-t_*+\tau,\tau)]\,\mathrm{d}\tau,$$

and repeating the operation

$$\frac{\partial^2 \psi}{\partial t_*^2} = \Gamma(\tilde{r},t_*) + \frac{1}{2}\int_0^{t_*} \left[\frac{\partial \Gamma}{\partial \alpha}\bigg|_{\alpha=\tilde{r}+t_*-\tau} - \frac{\partial \Gamma}{\partial \beta}\bigg|_{\beta=\tilde{r}-t_*+\tau}\right]\mathrm{d}\tau,$$

which, by (B 1), may be written as

$$\frac{\partial^2 \psi}{\partial t_*^2} = \Gamma(\tilde{r},t_*) + \frac{\partial^2 \psi}{\partial \tilde{r}^2},$$

which may be made to coincide with (7.7*a*) by the substitution $\phi_2 = -\psi/\tilde{r}$ as in (7.14*a*). In the further manipulations involving the function Γ in §7 it is helpful to bear in mind that it is an odd function of $\tilde{r}$, as follows from its definition (7.8).

REFERENCES

COLE, R. H. 1948 *Underwater Explosions*. Princeton University Press (reprinted by Dover 1965).

EPSTEIN, D. & KELLER, J. B. 1971 Expansion and contraction of planar, cylindrical, and spherical underwater gas bubbles. *J. Acoust. Soc. Am.* **52**, 975–980.

FLYNN, H. G. 1975 Cavitation dynamics I. A mathematical formulation. *J. Acoust. Soc. Am.* **57**, 1379–1396.

FUJIKAWA, S. & AKAMATSU, T. 1980 Effects of the non-equilibrium condensation of vapor on the pressure wave produced by the collapse of a bubble in a liquid. *J. Fluid Mech.* **97**, 481–512.

GILMORE, F. R. 1952 The collapse and growth of a spherical bubble in a viscous compressible liquid. *California Institute of Technology Hydrodynamics Laboratory, Rep.* 26–4.

HERRING, C. 1941 Theory of the pulsations of the gas bubble produced by an underwater explosion. *OSRD Rep.* 236.

HICKLING, R. & PLESSET, M. S. 1964 Collapse and rebound of a spherical bubble in water. *Phys. Fluids* **7**, 7–14.

KAPLUN, S. 1967 *Fluid Mechanics and Singular Perturbations* (ed. P. A. Lagerstrom, L. N. Howard & C. S. Liu), pp. 43–60. Academic.

KELLER, J. B. & KOLODNER, I. I. 1956 Damping of underwater explosion bubble oscillations. *J. Appl. Phys.* **27**, 1152–1161.

KELLER, J. B. & MIKSIS, M. 1980 Bubble oscillations of large amplitude. *J. Acoust. Soc. Am.* **68**, 628–633.

LAGERSTROM, P. A. & CASTEN, R. G. 1972 Basic concepts underlying singular perturbation techniques. *SIAM Rev.* **14**, 63–120.

OBERMEIER, F. 1976 The application of singular perturbation methods to aerodynamic sound generation. In Lecture Notes in Mathematics, vol. 596, pp. 400–418, Springer.

PROSPERETTI, A. & LEZZI, A. 1986 Bubble dynamics in a compressible liquid. Part 1. First-order theory. *J. Fluid Mech.* **168**, 457–478.

RATH, H. J. 1980 Free and forced oscillations of spherical gas bubbles and their translational motion in a compressible fluid. In *Cavitation and Inhomogeneities in Underwater Acoustics* (ed. W. Lauterborn), pp. 64–71. Springer.

TILMANN, P. M. 1980 Nonlinear sound scattering by small bubbles. In *Cavitation and Inhomogeneities in Underwater Acoustics* (ed. W. Lauterborn), pp. 113–118. Springer.

TOMITA, Y. & SHIMA, A. 1977 On the behavior of a spherical bubble and the impulse pressure in a viscous compressible liquid. *Bull. JSME* **20**, 1453–1460.

TRILLING, L. 1952 The collapse and rebound of a gas bubble. *J. Appl. Phys.* **23**, 14–17.